



WiLife: Long-Term Daily Status Monitoring and Habit Mining of the Elderly Leveraging Ubiquitous Wi-Fi Signals

SHENGJIE LI, Peking University, Beijing, China and JD.com, Beijing, China

ZHAOPENG LIU, Peking University, Beijing, China

QIN LV, University of Colorado Boulder, Boulder, CO, USA

YANYAN ZOU, JD.com, Beijing, China

YUE ZHANG, Peking University, Beijing, China

DAQING ZHANG, Peking University, Beijing, China and Institut Polytechnique de Paris, Paris, France

The global aging demographic underscores the imperative for continuous in-home monitoring of the empty-nest elderly, ensuring their safety and well-being. The widespread deployment of Wi-Fi infrastructure has paved the way to monitor the elderly in a non-intrusive and privacy-preserving manner. Numerous studies have explored the potential of utilizing Wi-Fi signals to address urgent life safety concerns such as fall detection and vital sign monitoring. However, apart from these acute safety issues, the early detection of potential disease symptoms and managing the progression of chronic diseases are also crucial for elderly care, which calls for long-term and continuous monitoring of the elderly's daily routines. Unfortunately, challenges like continuous activity segmentation and location/orientation dependencies have hindered the implementation of a long-term, around-the-clock activity monitoring system for the elderly. This work introduces "WiLife," a cutting-edge Wi-Fi-based framework for continuous monitoring of the elderly's spatio-temporal daily status information. Specifically, WiLife adopts a strategy of partitioning living spaces into functional *areas* and categorizing daily activities into atomic *states*. By encapsulating daily life status into a unique series of triple unit format: $\langle Time, Area, State \rangle$, WiLife is able to offer valuable insights into when, where, and how activities occur. Field implementations spanning 1,080 hours (45 days \times 24 hours) in real-world home environments highlight WiLife's exceptional capability in understanding individual living habits and timely detection of irregularities.

CCS Concepts: • **Applied computing** → **Health care information systems**; • **Human-centered computing** → **Ubiquitous and mobile computing**;

Additional Key Words and Phrases: Wi-Fi, Wireless sensing, health monitoring, elderly care

This work is supported by NSFC A3 Foresight Program Grant 62061146001.

Authors' Contact Information: Shengjie Li (corresponding author), Peking University, Beijing, China and JD.com, Beijing, China; e-mail: lishengjie_java@126.com; Zhaopeng Liu, Peking University, Beijing, China; e-mail: liuzp@pku.edu.cn; Qin Lv, University of Colorado Boulder, Boulder, CO, USA; e-mail: qin.lv@colorado.edu; Yanyan Zou, JD.com, Beijing, China; e-mail: zoe.yyzou@gmail.com; Yue Zhang, Peking University, Beijing, China; e-mail: zhangyue.pro@gmail.com; Daqing Zhang, Peking University, Beijing, China and Institut Polytechnique de Paris, Paris, France; e-mail: dqzhang@sei.pku.edu.cn.

Permission to make digital or hard copies of all or part of this work for personal or classroom use is granted without fee provided that copies are not made or distributed for profit or commercial advantage and that copies bear this notice and the full citation on the first page. Copyrights for components of this work owned by others than the author(s) must be honored. Abstracting with credit is permitted. To copy otherwise, or republish, to post on servers or to redistribute to lists, requires prior specific permission and/or a fee. Request permissions from permissions@acm.org.

© 2025 Copyright held by the owner/author(s). Publication rights licensed to ACM.

ACM 2637-8051/2025/1-ART10

<https://doi.org/10.1145/3689373>

ACM Reference format:

Shengjie Li, Zhaopeng Liu, Qin Lv, Yanyan Zou, Yue Zhang, and Daqing Zhang. 2025. WiLife: Long-Term Daily Status Monitoring and Habit Mining of the Elderly Leveraging Ubiquitous Wi-Fi Signals. *ACM Trans. Comput. Healthcare* 6, 1, Article 10 (January 2025), 29 pages.

<https://doi.org/10.1145/3689373>

1 Introduction

The global population is undergoing a rapid aging process, and the population of elderly individuals continues to increase [50]. Providing adequate care for these elderly poses substantial challenges for many countries, especially in light of limited healthcare resources.¹ In this context, a majority of the elderly express a preference for aging in place, i.e., living in their own homes with comfort and independence.² Especially for elderly patients with chronic diseases, the long recovery period often means that their rehabilitation predominantly takes place in their homes [8]. However, physiological aging and pathological changes will cause various unsafe situations for these elderly people, such as gradual reduction in activity, gradual lethargy, and inability to stand up after falling [32]. These conditions seriously threaten the health and safety of the elderly. Therefore, delivering healthcare support for these aging-at-home elderly is becoming an urgent societal imperative, which has motivated researchers to propose various activity sensing technologies for elderly care [10, 13, 15, 17, 27, 33, 38, 65]. These technologies can be broadly categorized into two types: device-based and device-free methods. Device-based methods require the elderly to wear certain types of sensors all day. The sensors only work when they are properly worn and powered. Wearing and charging the sensors regularly is cumbersome, especially for the elderly at home. Among device-free technologies, computer vision-based technologies are usually accurate but pose severe privacy concerns [13, 65].

Recently, with the widespread deployment of Wi-Fi infrastructure, Wi-Fi-based contactless sensing solutions have been developed [18, 24, 26, 35, 36, 42, 51, 52, 54–58, 63, 66, 67], enabling activity sensing in a ubiquitous and privacy-preserving manner. These systems have shown significant progress in addressing the safety concerns in home care, especially in critical applications such as fall detection and vital sign monitoring. Besides such acute life safety issues, long-term and round-the-clock monitoring of the elderly's daily activities is also of paramount importance. Continuous observation of the elderly's daily routines over extended periods can provide valuable insights into their living habits and overall health conditions, allowing for early detection of potential health issues and timely intervention if their condition deteriorates. For example, changes in daily habits can be indicative of mental health issues such as depression, dementia, or the onset of Alzheimer's [47]. Intuitively, Wi-Fi-based activity recognition methods could be an ideal way to continuously monitor and identify the diverse daily activities of the elderly due to ubiquitous Wi-Fi signals [26, 54, 58, 63]. The majority of existing activity recognition research follows a two-step process: first the signal stream into individual activities and then classifying these activities. They typically operate under two assumptions: (1) Each activity starts and ends with a set of pre-defined rules (e.g., remaining still before and after an activity) [24, 34, 62], and (2) the location and motion orientation of the sensing subject should remain constant to obtain a stable signal pattern for activity classification [68]. However, in real daily life, the activities of the elderly are carried out continuously without any accurate anchor marking the start and end of each activity, in particular, quite some of the activities are interleaved, making it very difficult to segment automatically. Furthermore, there are unlimited kinds of activities and each activity can be performed at different locations with different orientations, further increasing the complexity of the problem. Due to these real-world challenges, existing activity recognition systems are insufficient to address the long-term care needs of

¹"World population aging: 2020" (the United Nations).

²"Aging in Place: US State Survey of Livability Policies and Practices."

the elderly. Long-term, continuous, real-time monitoring of the daily activities of elderly care remains a significant challenge in the field of wireless sensing.

Harnessing the potential of ubiquitous Wi-Fi signals, this article redefines the fundamental nature of at-home eldercare and addresses the associated challenges from a fresh perspective. One crucial insight lies in the understanding that the living habits and health conditions of the elderly are closely related to spatio-temporal change patterns in their daily life status. For instance, behaviors such as eating on schedule, regular bathroom use, regular walking, and sufficient sleep serve as indicators of the elderly maintaining healthy lifestyles. Conversely, a sudden decrease in activity or frequent nighttime bathroom visits may signify health deterioration or the emergence of abnormal conditions [45]. Inspired by this insight, rather than attempting to recognize each individual activity, we focus on discerning the specific condition or posture of the person being monitored (i.e., behavioral states) and formulate the problem as continuous monitoring of an elder person's daily life status (i.e., $\langle \text{Time}, \text{Area}, \text{State} \rangle$), and mining of the elderly's daily habits. However, in practice, obtaining such spatio-temporal daily status and leveraging it for daily habit mining is also challenging due to the following reasons:

- *Precise positioning of functional areas.* Understanding the precise area in which the target is located, such as the kitchen or bathroom, provides a crucial semantic context for monitoring the daily life status of at-home elderly individuals. The precise positioning of functional areas (e.g., bedroom vs. bathroom) requires accurately determining which side of the area boundary line the target is located on. However, with a 90th percentile localization error of 2 m [20], traditional Wi-Fi-based localization systems struggle to precisely pinpoint the specific functional area where the target is situated.
- *Abstraction and distinction of behavioral states.* In addition to identifying spatial areas, it is equally crucial to ascertain the behavioral states within a specific area at a given time to depict the daily life status accurately. Note that the elderly can carry out a variety of daily activities in their daily lives, such as eating, sleeping, watching TV, and cooking. The challenge at hand is how to abstract these activities into a few enumerable behavioral states and then effectively differentiate between these behavioral states using Wi-Fi signals.
- *Long-term habit tracking and timely anomaly detection.* After deriving the triple units $\langle \text{Time}, \text{Area}, \text{State} \rangle$ of daily status, there remains a gap between the triple units and the elderly's daily habit. Such triple units, given their granular level of abstraction, cannot directly correspond to easily identifiable habits. Thus, mining individual daily habits from a sequence of these triple units and identifying anomalies present further challenges.

Our work is dedicated to addressing these technical challenges in order to facilitate long-term daily status monitoring of the elderly. Firstly, we utilize the walls and their extensions as well-defined boundaries, which naturally divide an apartment into several functional areas (e.g., kitchen, bedroom, bathroom). By continuously determining whether a person is inside or outside the various walls in a house, we can consistently acquire precise area information about the sensing target. Regarding the distinction of behavioral states, we have observed that diverse activities can be categorized based on the movement range of activities, which can be abstracted into three kinds of high-level behavioral states (hereinafter referred to as the “state”): (1) *still*: when the person is in an almost stationary state such as sleeping; (2) *in-situ moving*: when the person is doing *in-situ* activities like cooking and washing; and (3) *walking*: when the person is moving from one place to another place. By utilizing the Doppler effect to detect the range of movement, we can effectively segment continuous moving activities into these three distinct atomic states. Upon deriving the triple units $\langle \text{Time}, \text{Area}, \text{State} \rangle$ to depict an individual's daily life status, we further develop a habit vector constructed from observations of numerous triple units, offering a detailed overview of a person's daily activities spanning a 24-hour cycle. Moreover, we introduce the “Living Index,” a tailored indicator designed to quantify the regularity and consistency of an individual's daily routine. The key contributions of this work can be summarized as follows:

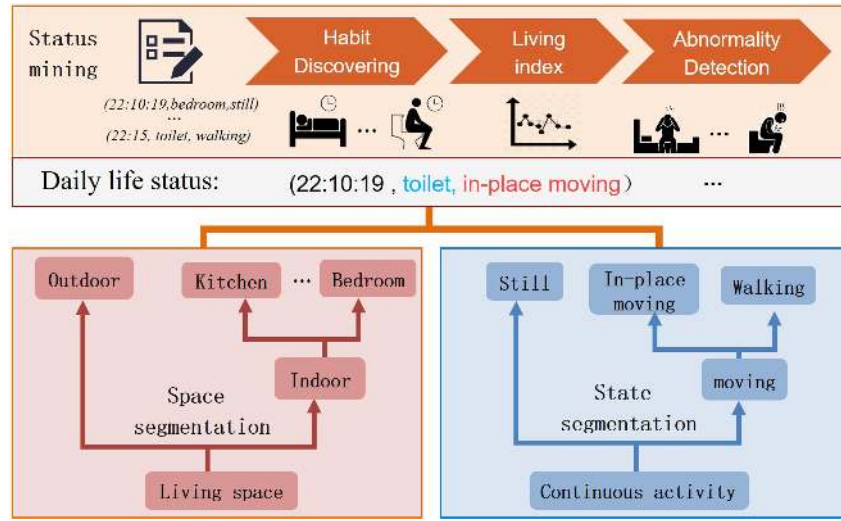


Fig. 1. Overview of WiLife. (The WiLife platform mainly consists of three modules: a space segmentation module, a state segmentation module, and a daily life status mining module.)

- We present a novel and practical Wi-Fi-based framework designed specifically for long-term elderly care. This framework conceptualizes long-term care as the continuous monitoring of an elderly individual's spatio-temporal daily status, represented through a series of unique triple units: $\langle \text{Time}, \text{Area}, \text{State} \rangle$.
- We propose to abstract diverse and innumerable daily activities into three high-level enumerable behavioral states. By continuously analyzing the Wi-Fi signal stream, we uniquely capture not only the behavioral state details but also the precise area information, providing a comprehensive insight into the when, where, and how of a subject's activities.
- We have observed numerous triple units over long periods of time and developed a “habit vector” to summarize a person's daily activities spanning a 24-hour cycle. To detect behavioral anomalies in time, we also design an effective indicator to quantify the regularity and consistency of an individual's daily routine.
- We have implemented WiLife and deployed it in two real-world home settings. With 15 volunteers conducting their daily lives in these environments, the system ran continuously for more than 1,080 hours (45 days \times 24 hours) and generated real-time and rich statistics about each inhabitant, demonstrating WiLife's excellent ability to understand individual living habits and timely detection of irregularities.

A demonstration video of our spatio-temporal segmentation methods and the WiLife Web site can be accessed online.³ It is worth mentioning that WiLife has been deployed in a nursing home with 12 Alzheimer's patients, providing continuous monitoring of their daily routines and promptly detecting any abnormal situations.

2 WiLife

2.1 Platform Overview

To capture the spatio-temporal daily status information, WiLife proposes a strategy of partitioning living spaces into functional *areas* and categorizing daily activities into atomic *states*. It mainly consists of three modules as shown in Figure 1: (1) space segmentation module, (2) state segmentation module, and (3) daily life status mining module.

³<https://youtu.be/4HDo1Td6hbk>

The Space Segmentation module is designed to accurately position the sensing target within a specific area by delineating distinct boundaries, termed as “sensing boundaries,” within the living space. This module capitalizes on the natural barriers formed by walls and their extensions to segment the entire space. Initially, it ascertains whether the subject being sensed is indoors or outdoors by continuously evaluating their position relative to the exterior walls of the dwelling. When the subject is detected indoors, the module integrates their relative position with respect to various interior walls to determine the precise *Area* in which the individual is currently located.

The State Segmentation module is designed to obtain the behavioral state information by segmenting the continuous activities into atomic states. To differentiate these states, the module harnesses the Doppler effect observed in Wi-Fi signals, which is influenced by human movement. Then the Doppler effect is used to characterize the range of motion, which can effectively segment continuous motion activities into three kinds of atomic states (i.e., *still*, *in-situ moving*, *walking*).

By leveraging the capabilities of the two aforementioned modules, we can derive a triple unit $\langle \text{Time}, \text{Area}, \text{State} \rangle$ to depict an individual’s daily life status. Then we design the “Daily Life Status Mining” module to bridge the gap between the triple unit and the elderly’s daily habits. By aggregating the triple units over a period, we can formulate a “habit vector” that represents an individual’s activity over a 24-hour span. Furthermore, we’ve introduced a “Living Index” derived from this habit vector, which quantifies the consistency of an individual’s daily routine. Monitoring fluctuations in this index allows us to promptly detect any irregularities or deviations from their norm.

2.2 Basis for Wi-Fi Sensing

Wi-Fi configurations typically involve a transmitter–receiver pair. The signal that the receiver captures is a composite of signals that have taken both direct and reflected paths. These reflected paths can be due to humans, walls, and other objects in the vicinity, leading to what is known as multi-path propagation. As a result, these received signals inherently carry information that highlights the impact of human moving within that environment. If we consider the signal propagation environment (including ambient objects and human) as a wireless channel, the Wi-Fi **Channel State Information (CSI)** exactly depicts such a wireless channel [22]. It can be expressed as [64]

$$H(f, t_0 + t) = e^{j\theta_{offset}} (A_s e^{j\phi_s} + \sum_{d=1}^D \alpha_d(t_0 + t) e^{j\phi_d(t_0+t)}), \quad (1)$$

where f is the carrier frequency of the Wi-Fi signal, $e^{j\theta_{offset}}$ is random phase offset due to asynchronous hardware [40], $A_s e^{j\phi_s}$ is merged static signal (i.e., reflected by static objects such as walls or furniture), d is the number of human reflected signals, $\tau_d(t_0 + t)$ is the propagation delay of the d th signal at time $t_0 + t$, $\alpha_d(t_0 + t)$ is the amplitude attenuation. Such CSI can be obtained from multiple Orthogonal Frequency Division Multiplexing sub-carriers and multi-antennas.

To eliminate the random phase offset, we can apply the conjugate multiplication between CSI on two antennas [37] and then derive a new conjugate-multiplying CSI as shown in Equation (2):

$$H_1(f, t_0 + t) \cdot H_2^*(f, t_0 + t) = \underbrace{A_{s_1} A_{s_2} e^{j(\phi_{s_1} - \phi_{s_2})}}_1 + \underbrace{A_{s_1} \sum_{d=1}^D \alpha_d(t_0) e^{-j(\phi_d^1(t_0+t) + \phi_{s_1})}}_2 + \underbrace{A_{s_2} \sum_{d=1}^D \alpha_d(t_0) e^{j(\phi_d^2(t_0+t) - \phi_{s_2})}}_3. \quad (2)$$

The new conjugate-multiplying CSI is composed of three components, where the first component is a constant and does not change over time, and the second and the third components (i.e., including human reflected signals) would change corresponding to the human target movement.

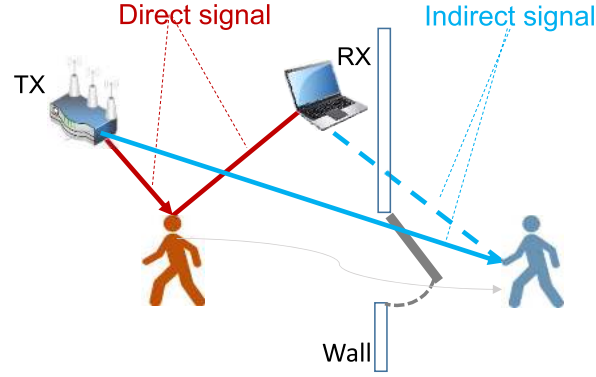


Fig. 2. Illustration of direct and indirect signals when human moves inside-wall and outside-wall, respectively.

2.3 Space Segmentation

To accurately position the sensing target within a specific area, this module capitalizes on the natural barriers formed by walls and their extensions to segment the entire space. The key observation is that the amplitude of signals directly reflected by a person (i.e., direct signals) attenuates gradually in an open space, while the signal amplitude attenuates dramatically when the person moves behind a wall (i.e., direct signals become indirect through-wall signals), as illustrated in Figure 2.

To characterize such signal amplitude for inside-wall and outside-wall discrimination, a metric $\sigma(t_0)$ can be obtained by conjugate-multiplying CSI [37]. Suppose there are M conjugate-multiplying CSI samples within a short time window, we can construct a conjugate-multiplying vector:

$$\vec{S}(f, t_0) = [H_1(f, t_0)H_2^*(f, t_0), H_1(f, t_0 + \Delta t_1)H_2^*(f, t_0 + \Delta t_1), \dots, H_1(f, t_0 + \Delta t_M)H_2^*(f, t_0 + \Delta t_M)],$$

where $[0, \Delta t_1, \dots, \Delta t_M]$ is the sampling interval with respect to the sample of time t_0 . Then by subtracting the mean value of the vector $\vec{S}(t_0)$, we can remove the constant signal term in the conjugate-multiplying CSI and get a zero-mean vector $\vec{X}(f, t_0)$:

$$\vec{X}(f, t_0) = \vec{S}(f, t_0) - \overline{\vec{S}(f, t_0)}.$$

Assume variable $x(f, t_0 + \Delta t_k)$ is the k th element in vector $\vec{X}(f, t_0)$. Combined with Equation (2), we can express $x(f, t_0 + \Delta t_k)$ as

$$x(f, t_0 + \Delta t_k) = A_{s_1} \sum_{d=1}^D \alpha_d(t_0) e^{j\Psi_d(t_0 + \Delta t_k)} + A_{s_2} \sum_{d=1}^D \alpha_d(t_0) e^{j\Omega_d(t_0 + \Delta t_k)}.$$

Note that after the mean-subtract operation, the first static CSI part in conjugate-multiplying CSI has been removed. And $\Psi_d(t_0 + \Delta t_k)$, $\Omega_d(t_0 + \Delta t_k)$ are the mean-subtract phase. Then turning $x(f, t_0 + \Delta t_k)$ into complex representation, it can be expressed as

$$\begin{aligned} x(f, t_0 + \Delta t_k) &= R(t_0 + \Delta t_k) + iI(t_0 + \Delta t_k), \\ R(t_0 + \Delta t_k) &= A_{s_1} \sum_{d=1}^D \alpha_d(t_0) \cos(\Psi_d(t_0 + \Delta t_k)) + A_{s_2} \sum_{d=1}^D \alpha_d(t_0) \cos(\Omega_d(t_0 + \Delta t_k)), \\ I(t_0 + \Delta t_k) &= A_{s_1} \sum_{d=1}^D \alpha_d(t_0) \sin(\Psi_d(t_0 + \Delta t_k)) + A_{s_2} \sum_{d=1}^D \alpha_d(t_0) \sin(\Omega_d(t_0 + \Delta t_k)). \end{aligned}$$

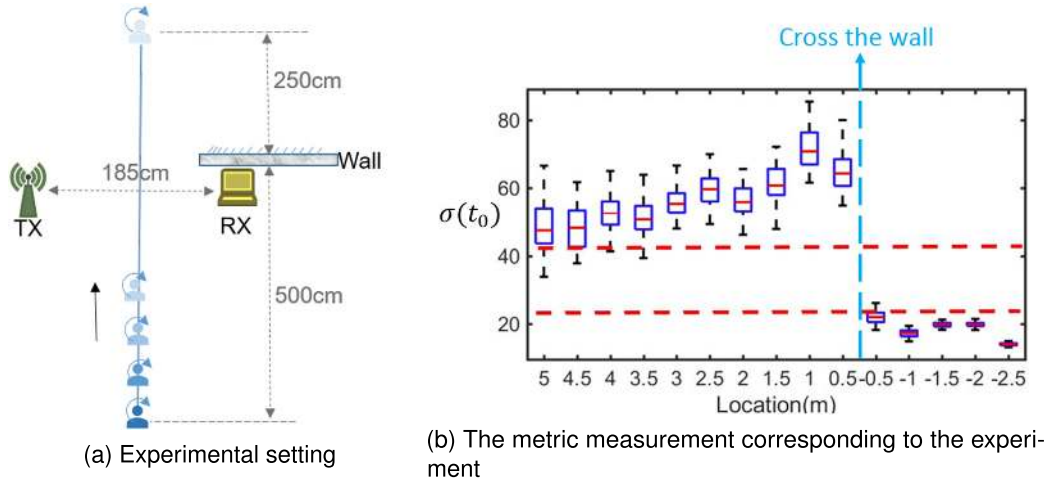


Fig. 3. (a) The experimental setting for the metric study; (b) results of metric measurement for signal discrimination between inside-wall and outside-wall scenarios.

$R(t_0 + \Delta t_k)$ and $I(t_0 + \Delta t_k)$ are the sum of two orthogonal parts, respectively. According to the Central Limit Theorem [12], the distribution of $R(t_0 + \Delta t_k)$ and $I(t_0 + \Delta t_k)$ shall follow a zero-mean normal distribution $R(t_0 + \Delta t_k) \sim N(0, \sigma(t_0)^2)$, $I(t_0 + \Delta t_k) \sim N(0, \sigma(t_0)^2)$, where $\sigma(t_0)$ is expressed as

$$\sigma(t_0) = \sqrt{(A_{s_1}^2 + A_{s_2}^2) \sum_{d=1}^D \alpha_d^2(t_0)/2} = \sqrt{\frac{1}{2M} \sum_{k=1}^M |x(f, t_0 + \Delta t_k)|^2}, \quad (3)$$

where M is a set of conjugate-multiplying CSI samples within a short time window, and $x(f, t_0 + \Delta t_k)$ is the k th sample after subtracting the mean from the set M . And the variance parameter $\sigma(t_0)$ is referred to as the metric for through-wall discrimination due to the following properties:

- A_{s_1}, A_{s_2} are amplitudes of merged static signals on two antennas. In a specific environment, they are usually constant and do not change over time. The amplitude $\alpha_d(t_0)$ of dynamic signals depends on the attenuation of the path length and the occlusion of objects. Compared with direct signals, the amplitude of indirect signals significantly attenuates because of the wall's occlusion, which would introduce a significant change on $\alpha_d(t_0)$. After the square operation, this change will dominate $\sigma(t_0)$ and present a strong distinction between direct and indirect signals.

To validate the effectiveness of the metric, a volunteer walks along the bisector of the transceivers from inside the room to **Line of Sight (LoS)**, and then from LoS to outside, stopping at each interval of 0.5 m as shown in Figure 3(a). At each stopped location, the volunteer rotates around in place for 20 seconds to record the CSI data. Correspondingly, Figure 3(b) shows the metric measurement, in which crossing the wall boundary (i.e., moving from inside the wall to outside the wall) would result in a sudden decrease in the value of $\sigma(t_0)$. Such a sudden change of $\sigma(t_0)$ can thus be utilized to discriminate between inside-wall and outside-wall scenarios.

Utilizing the exterior walls of the house and extracted sensing metrics, we can easily differentiate between indoor and outdoor scenes. To further achieve the precise area positioning of the sensing subject indoors, we here fully take advantage of multiple interior walls in the house and extract the $\sigma(t_0)$ from multiple devices. As shown in Figure 4, we can employ multiple existing Wi-Fi transceiver pairs and indoor walls to divide the indoor space into several sub-areas. When the human target moves from one area to another, the direct/indirect signals

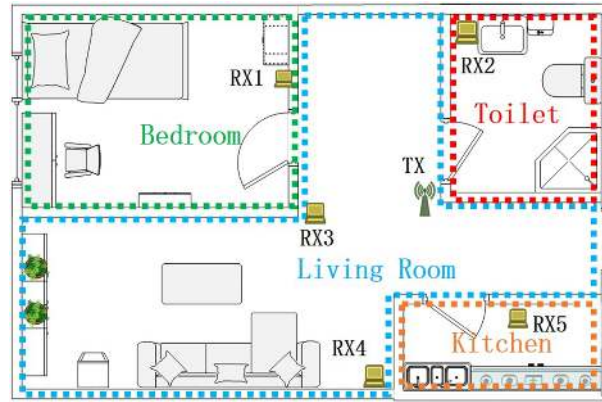


Fig. 4. Space segmentation with one transmitter and multiple receivers.

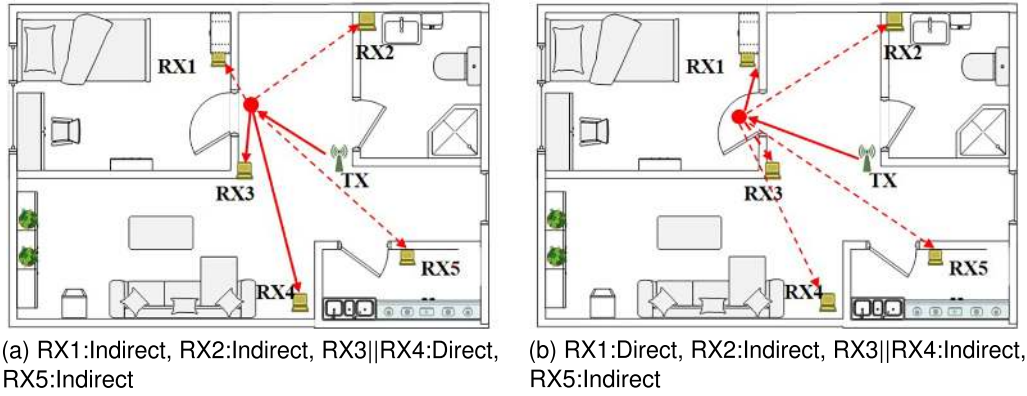


Fig. 5. Direct/indirect signal situations on receivers when people move in different areas.

from different transceivers change due to changes in wall blockage. Suppose the sensing target wants to move from the living room to the bedroom, the target needs to move close to the bedroom door (i.e., the boundary between the living room and the bedroom). As shown in Figure 5(a), when he/she gets close to the door but is still outside the bedroom, RX3 and RX4 receive direct signals, while other devices receive indirect signals. Right after he/she crosses the door and enters the bedroom, no direct signals reach RX3 or RX4 due to the blockage of the bedroom walls. Only RX1 receives direct signals as shown in Figure 5(b).

By extracting $\sigma(t_0)$ metrics from each receiver, we are able to obtain the direct/indirect signal situations of all receivers. If we encode the situations of having indirect or direct signals as 0 or 1 to each receiver, then an area transition diagram can be constructed offline as shown in Figure 6. For example, the indirect/direct signal encoding of the scenario in Figure 5(a) can be represented as $(RX1=0, RX2=0, RX3||RX4=1, RX5=0)$ (i.e., 0010) where “||” refers to “or.” When the encoding becomes $(RX1=1, RX2=0, RX3||RX4=0, RX5=0)$ (i.e., 1000) in Figure 5(b), the system will be triggered to update the area state of the sensing target as “inside the bedroom” as the new encoding matches one entry of the pre-defined transition encoding. Thus, once we have gathered real-time 0/1 encoding from all receivers, we can accurately determine a target person’s area using the Area-Transition-Diagram.

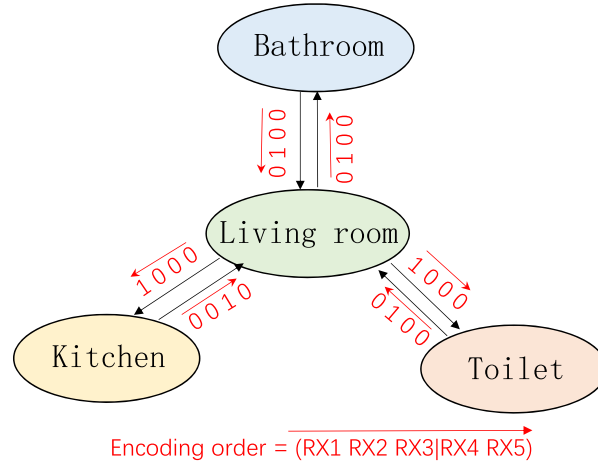


Fig. 6. Area-Transition-Diagram (the system updates the area state only if the new encoding matches one entry of the pre-defined transition encoding. Otherwise, it remains the area state unchanged).

2.4 State Segmentation

The state segmentation module is designed to obtain the behavioral state information by segmenting the continuous activities into atomic states. To differentiate these states, the module harnesses the Doppler effect observed in Wi-Fi signals, which is influenced by human movement. As shown in Figure 7(a), human movement can change the path length of the human reflection signal, and introduce a Doppler frequency shift to the received signal: $f_{Doppler} = \frac{f \cdot v_{path}}{c}$, where f is the carrier frequency of the signal, c is the light speed, and v_{path} is the path length change speed of the human reflected signal. Such Doppler shift will introduce the phase change of conjugate-multiplying CSI so that the phase $\phi_d^1(t_0 + t)$ in Equation (2) can also be expressed as

$$\phi_d^1(t_0 + t) = 2\pi f \left(\tau_{t_0} + \frac{v_{path} \cdot t}{c} \right). \quad (4)$$

Utilizing the signal separation algorithm [40] such as MUSIC or Capon to perform phase analysis on conjugate-multiplying CSI, we can obtain the path length change speed of the human reflected signal v_{path} to characterize the human movement. We call such path length change speed as *Doppler velocity*. Figure 7(b) shows the Doppler velocity obtained by a person walking. The value of v_{path} is 0 when the human is still and non-zero when the human is moving.

Considering various daily life activities, they can be categorized based on the movement range of activities and be abstracted into three kinds of high-level behavioral states: (1) still: when the person is mostly stationary such as sleeping; (2) *in-situ* moving: when the person is doing *in-situ* activities like cooking; and (3) walking: when the person is moving from one place to another place. The still state can be easily determined when the Doppler velocity is 0. The challenge is distinguishing between the walking and *in-situ* moving states. The key observation is shown in Figure 8. The *in-situ* moving states often occur in specific locations (e.g., cooking by the stove), where the position of the person changes irregularly in a small range. In contrast, the walking state would introduce a certain displacement in a certain direction, and the range of position changes is relatively large and regular. That is to say, within the same time window, the displacement changes of the *in-situ* moving state and the walking state will be different.

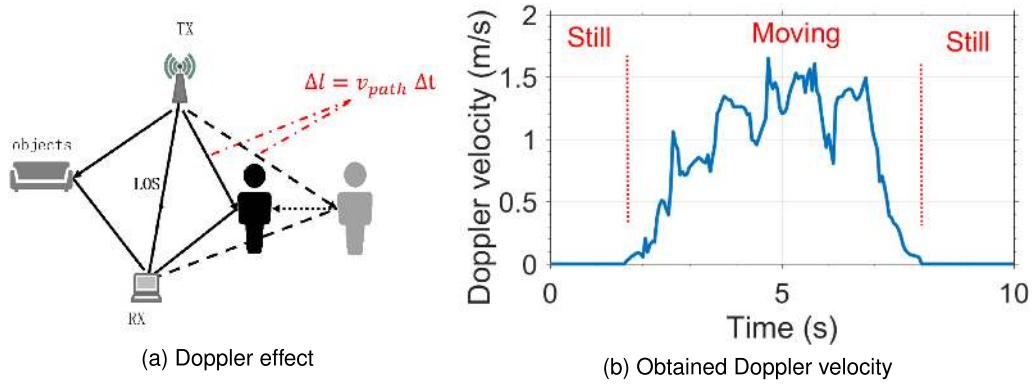


Fig. 7. (a) Doppler effect on Wi-Fi signal; (b) obtained Doppler velocity (the value of Doppler velocity is 0 when the human is still and non-zero when the human is moving).



Fig. 8. The difference between *in-situ* moving states and walking states.

Based on this observation, we use the Doppler velocities extracted from all receivers to obtain the approximate maximum displacement of the target in a short time window:

$$\max_Dis(t) = \max_{i=1}^N \int_{t-\Delta t}^t \frac{v_{path}^i}{2} dt, \quad (5)$$

where N is the number of receivers, and v_{path}^i is the Doppler velocity calculated from the i th receiver. To illustrate the maximum displacement of different activities, a volunteer has performed a series of short-term daily activities and the corresponding changes of displacement are illustrated in Figure 9. The displacement corresponding to the still state is 0, while the one corresponding to the walking state is significantly larger than that of the *in-situ* moving state. Therefore, the segmentation of continuous states can be performed according to the magnitude of such maximum displacement.

2.5 Daily Life Status Mining

2.5.1 Overall Description. Using the above spatio-temporal segmentation methods, we can derive a triple unit $\langle \text{Time}, \text{Area}, \text{State} \rangle$ to depict an individual's daily life status. By aggregating these triplets over a period, we can discern the daily routines of the subject. For instance, the 24-hour daily life status of a volunteer can be expressed as a radar chart shown in Figure 10. The different colors in the middle of the radar chart represent different functional areas, and the color changes over time indicate the area switching of the sensing target. The periphery of the radar chart shows the maximum displacement change over time, among which the long burr

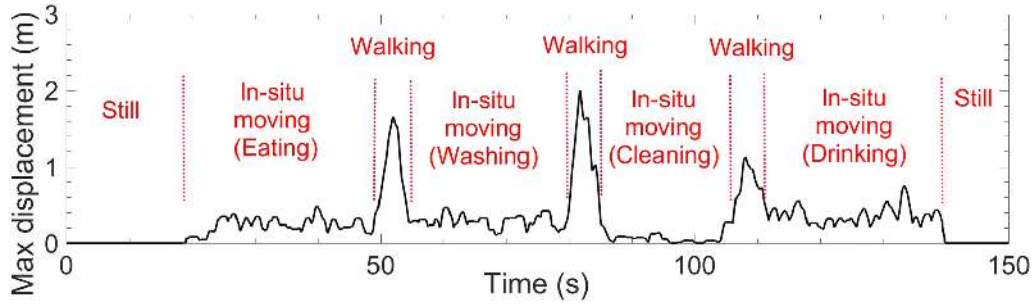


Fig. 9. The maximum displacement of different activities (the displacement corresponding to the still state is 0, while the one corresponding to the walking state is significantly larger than that of the *in-situ* moving state).

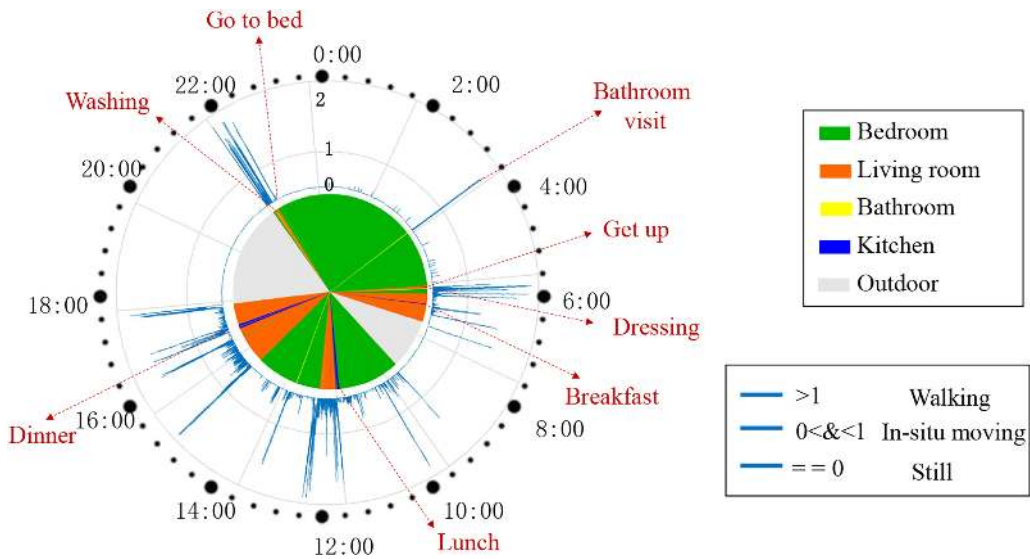


Fig. 10. One volunteer's daily life status over 24 hours (the different colors in the middle of the radar chart represent different functional areas, and the color changes over time indicate the area switching of the sensing target. The periphery of the radar chart shows the maximum displacement change over time, among which the long burr (> 1) is the walking time, the non-burr ($= 0$) is the still time, and the short burr ($0 < \& < 1$) is the *in-situ* moving time).

(> 1) is the walking time, the non-burr ($= 0$) is the still time, and the short burr ($0 < \& < 1$) is the *in-situ* moving time. Such a 24-hour overall description demonstrates changes in the volunteer's 24-hour area and state over time. For example, he went out twice, from 7:30 a.m. to 8:30 a.m., and from 18:00 to 22:00. When he was indoors, he stayed in the bedroom (colored in green) most of the time, and the infrequent area switching is often accompanied by walking. This example illustrates how we can identify a person's living habits based on the area and state information. Then, we will dig out the living habits of volunteers from areas and states, respectively.

2.5.2 Bedroom Habits. Figure 11 shows the real-life bedroom state change of two volunteers in 5 days. We mark the longest continuous time in the bedroom as dark green. At a high level, we can see that Volunteer1 spent more time in the bedroom than Volunteer2. However, the temporal distribution of Volunteer1 in the bedroom is relatively scattered, while the time spent by Volunteer2 in the bedroom is relatively concentrated. By reviewing the ground-truth video (camera recording), we found that both volunteers have the habit of working in the

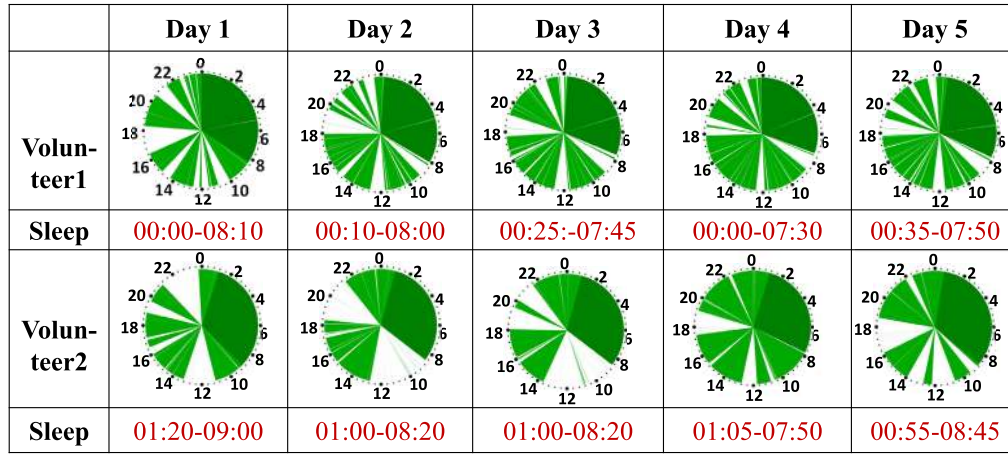


Fig. 11. Bedroom status over time (the real-life bedroom state change of two volunteers in 5 days. The longest continuous time in the bedroom is marked as dark green. We can see that Volunteer1 spent more time in the bedroom than Volunteer2).

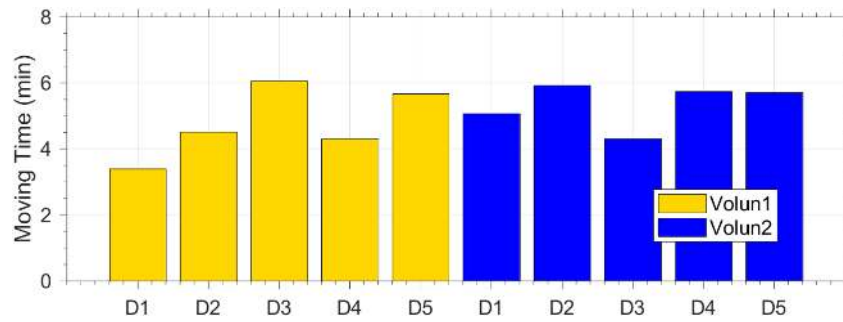


Fig. 12. Total time of moving during sleep. (The figure shows the time of body movement of the two volunteers during the sleeping period, indicating that both volunteers sleep normally.)

bedroom during the day, so the total time in the bedroom is longer. Since Volunteer1 (male) is more active and takes more breaks during work, his time in the bedroom is relatively scattered. In contrast, Volunteer2 (female) has a sedentary habit, and only gets up and leaves the bedroom when she goes to the bathroom or drinks water, so her time in the bedroom is relatively concentrated. Furthermore, when combined with the actual timestamps, we can see that the longest time period in the bedroom basically coincides with the sleep time. Therefore, it can be inferred that the bedtime of Volunteer1 is around midnight and the wake-up time is around 8:00 a.m. In contrast, Volunteer2 sleeps later than Volunteer1, usually going to bed around 1:00 a.m. and waking up between 8:00 a.m. and 9:00 a.m.

Further zooming in, we can observe a white line between 4:00 a.m. and 6:00 a.m. during Volunteer1's sleeping period, which actually corresponds to the volunteer's habit of getting up at night. Moreover, if a person has insomnia or dreams a lot at night, his/her movement would increase significantly during sleep. Therefore, by checking the movement information during sleep, our platform can also infer sleep quality. Figure 12 shows the time of body movement of the two volunteers during the sleeping period, indicating that both volunteers sleep normally.

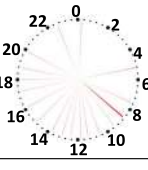
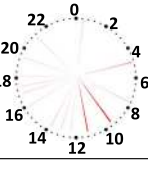
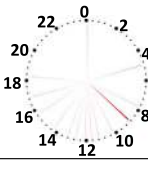
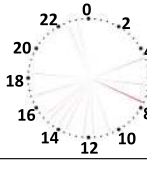
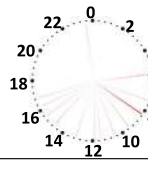

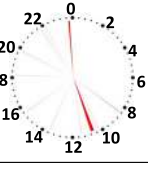
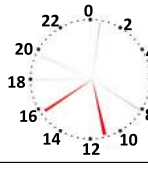

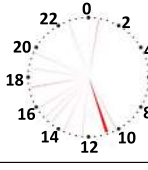
	Day 1	Day 2	Day 3	Day 4	Day 5
Volunteer1					
Toilet	08:30	09:40	08:45	07:50	08:10
Volunteer2					
Toilet	11:15	10:50	11:05	10:50	11:10

Fig. 13. Bathroom status over time (Volunteer1 appeared in the bathroom more often than Volunteer2. Combined with the time clock, we can infer that long time span may correspond to the volunteers' bowel movements).

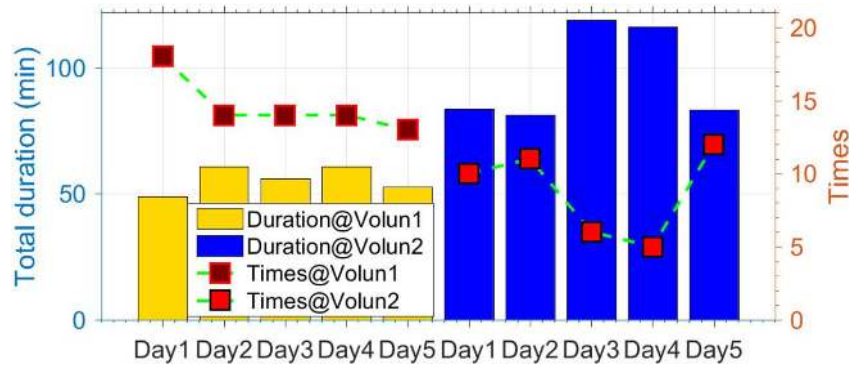


Fig. 14. Number of times and duration in the bathroom (the number of times the two volunteers go to the bathroom each day is within a reasonable range. Volunteer1 goes to the bathroom more frequently than Volunteer2, while Volunteer2 spends relatively more time in the bathroom than Volunteer1).

2.5.3 Bathroom Habits. Similarly, the real-life bathroom state change of two volunteers in 5 days is shown in Figure 13. In general, Volunteer1 appeared in the bathroom more often than Volunteer2. Examining the width of the red lines, we can identify periods of longer time span in the bathroom. Combined with the time clock, we can infer that these time periods may correspond to the volunteers' bowel movements, which are also verified by the volunteers. As demonstrated by the volunteers' data analysis results, our system can infer participants' bowel movement patterns in terms of time and duration, which can be particularly useful for eldercare.

More broadly, the frequency and duration of participants' bathroom use can reflect important health information. For example, how often a person goes to the bathroom every day reveals his/her body's metabolism. Therefore, our platform counts the total number of times each participant goes to the bathroom in a day and the total amount of time spent in the bathroom, as shown in Figure 14. It can be seen that the number of times the two volunteers go to the bathroom each day is within a reasonable range. Volunteer1 goes to the bathroom more frequently than Volunteer2, while Volunteer2 spends relatively more time in the bathroom than Volunteer1.

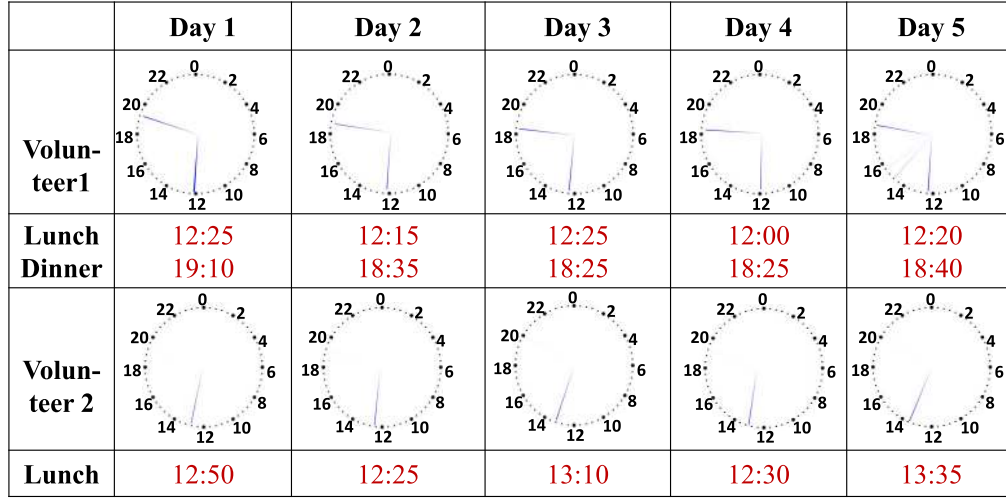


Fig. 15. Kitchen status over time (the most obvious blue line in the figure indicates that the volunteers were in the kitchen for a relatively long time. Combined with the time clock, we can infer that these blue lines correspond to the volunteers' three meals in a day).

2.5.4 Kitchen Habits. Cooking (and sometimes eating) often occurs in the kitchen. Regular entry and exit of the kitchen (dining room) are closely related to the periodicity of eating. Figure 15 shows the kitchen status of two volunteers over time for 5 days. The most obvious blue line in the figure indicates that the volunteers were in the kitchen for a relatively long time. Combined with the time clock, we can infer that these blue lines correspond to the volunteers' three meals in a day. From the multi-day display, we can see that Volunteer1 has the habit of eating lunch (around noon) and dinner (between 18:00 and 19:00) at home. In contrast, Volunteer2 only has a late lunch between 12:30 and 13:00.

2.5.5 Human Vitality. Our analysis above has revealed the relationship between daily habits (i.e., daily life status) and the area information. Furthermore, the state information is closely related to human life habits and physical health. The daily moving states (*in-situ* moving and walking) of the elderly reflect their basic daily vitality level [41], and the walking state is related to the motion ability of the elderly. Therefore, the proportions of moving time and walking time in a day are important indicators to measure an elder's daily vitality. Figure 16 shows the percentage of time that the two volunteers spent on moving and walking during each day (7:00–23:59). From the percentage values, we can see that the two volunteers spent most of the day in a still state, and only about 5% of their time is spent on moving while walking time is even less.

2.5.6 Living Index. By analyzing the daily life status captured by WiLife, we have unearthed a series of important features about the target life habits. Combined with long-term daily life status and expert knowledge, we can construct a habit vector to describe the target's 24-hour life condition as shown in Figure 17. The habit vector is a quantitative representation of an individual's daily activities, encoding the frequency, duration, and regularity of different activity categories. Mathematically, it is defined as a vector $X_d = [x_{d1}, x_{d2}, \dots, x_{dn}]$, where h_{di} represents a quantified measure of an activity type i on day d . When we consider multiple days, an array of habit vectors forms a habit matrix as Equation (6), which encapsulates the routine of an individual over a longer time span. This matrix serves as a comprehensive descriptor of the person's habits:

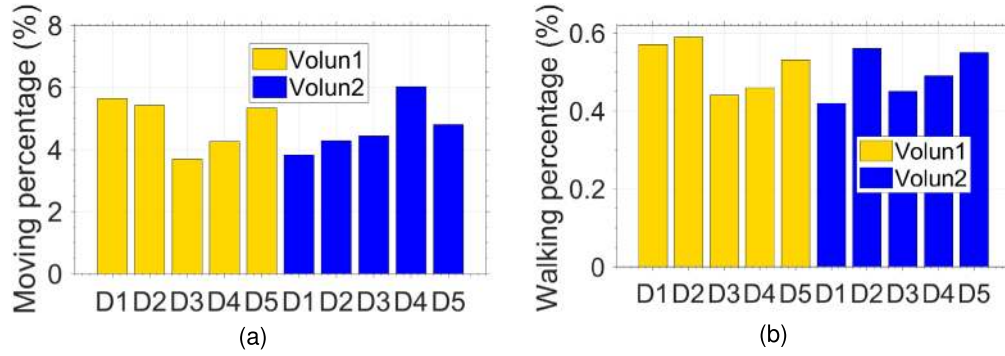


Fig. 16. Percentage of moving (a) and walking time (b). The two volunteers spent most of the day in a still state, and only about 5% of their time is spent on moving while walking time is even less.

Vector	The way of extraction	Meaning
23:00	The start time of the longest and highest proportion of the bedroom time period (after merge short interval)	Approximate time to sleep
08:00	The start time of the longest bedroom time period (after merging short interval) && this period has highest proportion of the still state	Approximate time to get up
4(min)	The total moving during above sleep period	Moving time during sleep (Sleep quality)
05:00	Time of first bathroom visit during above sleep period	First wake up time at night
1	Times of bathroom visit during above sleep period	Times for bathroom at night
10:00	Start time of the longest bathroom period && this period has highest proportion of still state	Start time of toileting
4(min)	Start time of the longest bathroom period with the highest proportion of still state	Duration of toileting
16	Total times of bathroom visit	Times of using bathroom
09:15	Start time of in-situ state in the kitchen for more than 10 minutes && Before 10:00	Breakfast
12:30	Start time of in-situ state in the kitchen with a duration of more than 10 minutes && Between 11:00-15:00	Lunch
18:40	Start time of in-situ state in the kitchen with a duration of more than 10 minutes && Between 16:00-20:00	Dinner
6(%)	Moving time percentage during the day(07:00-23:59)	Basic vitality
0.5(%)	Walking time percentage during the day(07:00-23:59)	Vitality

Fig. 17. Feature extraction of living habits.

$$C = \begin{bmatrix} 00:00 & 00:10 & \cdots & 00:35 \\ 08:10 & 08:00 & \cdots & 07:50 \\ \vdots & \vdots & \ddots & \vdots \\ 0.57 & 0.59 & \cdots & 0.53 \end{bmatrix}. \quad (6)$$

When a new day ends, we can get the habit vector for this day. In other words, based on the distance between the habit matrix and the habit vector formed on this day, we can describe the regularity of the new day's life status. Since Mahalanobis distance [44] is applicable to variables with different measures or sample distributions, we use Mahalanobis distance to quantify the distance between the new habit vector X and the habit matrix C ,

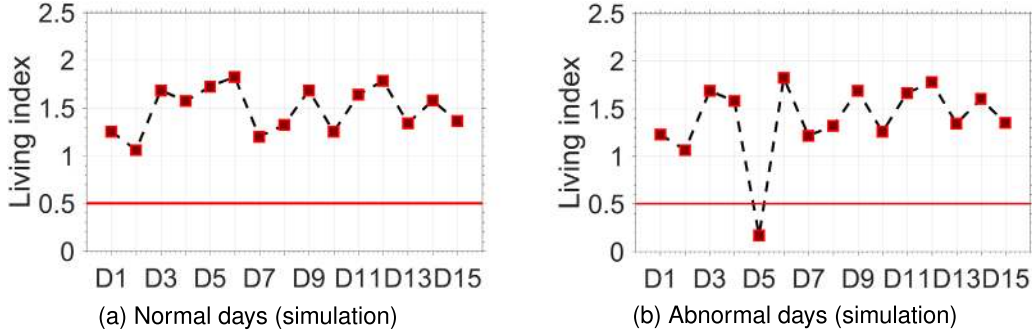


Fig. 18. (a) Living index of normal 15 days (simulation). (b) Living index with an abnormal day (simulation). We can set $LivingIndex = 0.5$ as the threshold (red line) to successfully distinguish between normal and abnormal days.

referred to as *living index*:

$$LivingIndex = \frac{\epsilon}{(X - m)^T \cdot C^{-1} \cdot (X - m)}, \quad (7)$$

where ϵ is a fixed constant, X is the habit vector corresponding to the new day, C is the habit matrix, m is the mean vector of C , and $(X - m)^T \cdot C^{-1} \cdot (X - m)$ represents the calculation of Mahalanobis distance. If the *LivingIndex* is within a certain threshold, the day is considered regular; otherwise, it may indicate an irregularity or a potential shift in the person's routine.

2.5.7 Anomaly Detection. Based on the characteristics of the normal distribution of each variable in the habit matrix in Section 2.5.6, we have generated a series of habit vectors under normal status through simulation. The habit vectors are divided into two groups. One group of vectors is used to form the habit matrix, and the remaining vectors are used for testing. For the test vector, we change each feature in the vector one by one to simulate the abnormality of the elderly by making the value of the feature deviate from the normal range. Then we comprehensively consider the living index of all normal and abnormal conditions and use a simple binary classifier to obtain the discrimination threshold (i.e., $LivingIndex = 0.5$). For example, Figure 18(a) shows the living index for several test vectors. When we change the number of wake-ups on the 5th day from 1 (average 1 time) to 4 times, the value of the living index will drop significantly below threshold, as shown in Figure 18(b), indicating an abnormal day.

When anomalies are detected, we can further determine the reason. Specifically, it is necessary to calculate the normalized distance between the habit vector of the abnormal day and all samples of the habit matrix as follows:

$$fDist_i = \frac{(fvalue_i - \mu)^2}{\sigma_i^2}, \quad (8)$$

where $fvalue_i$ is the value of the i th feature in the habit vector of the abnormal day, μ and σ^2 are the mean and variance values of the i th feature corresponding to the habit matrix. A larger normalized distance $fDist_i$ means there is a higher probability that the i th feature caused (or contributed to) the abnormality of that day.

3 Evaluation

3.1 Deployment Guidelines

Since the space segmentation module of WiLife leverages the walls or walls' extension to divide the space into different areas, the existence of walls plays an important role in WiLife deployment. WiLife makes use of the walls or walls' extension as the sub-area boundaries. For different layouts in different environments, the signal blockage

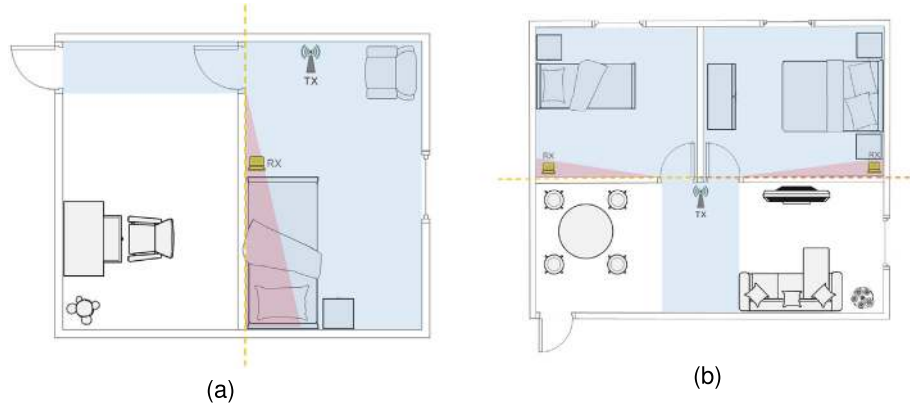


Fig. 19. (a) Transceivers deployment for single-boundary determination: blue area for transmitter deployment and red area for receiver deployment; and (b) transceivers deployment for multiple-boundary determination: blue area for transmitter deployment and red area for receivers deployment.

condition usually differs. As such, we need some guidance in terms of where to place the Wi-Fi transceivers given a specific indoor layout, either theoretically or empirically. Assume a space is divided by a common wall into two parts: inside-wall area and outside-wall area, wherein the inside-wall area serves as the sensing zone. Then, in order to leverage the wall or its extensions as a sensing boundary, the following two guidelines are summarized:

- (1) The Wi-Fi receiver is preferably deployed in the inside-wall area and not visible by a sensing target in the outside-wall area.
- (2) The Wi-Fi transmitter can be deployed either in the inside-wall area or outside-wall area, but it should be visible by a human target in the inside-wall area.

Based on the above guidelines, we can quickly select the appropriate places to deploy the transmitter and receivers, as shown in Figure 19(a), colored in blue and red. As for multi-room houses, it is also able to achieve multi-boundaries determination based on these two guidelines. As shown in Figure 19(b), by reasonably deploying one transmitter and multiple receivers, multiple boundaries can be formed by multiple walls in the house. Based on the tests in variously sized and configured spaces, we have found that for a typical household (50 m^2 to 200 m^2), precise localization within each functional area (e.g., kitchen, living room, bathroom) can be achieved by placing one RX in each area. Among these functional areas, TX can be placed in the central area connecting other areas (such as living room and corridor). In other words, one TX and RX with the same number of functional areas can achieve effective coverage of a typical household. For huge space larger than 200 m^2 , a single TX may not enough to cover the entire area due to the signal attenuation. In such cases, the central area can be further divided into two or more sub-areas, each with an additional TX and RX. For example, if the space is divided into x functional areas, and the central area of these functional areas is divided into y sub-areas, then we suggest deploying y TXs and $x + y - 1$ RXs to cover the entire space.

3.2 Evaluation Setup

To evaluate the performance of the WiLife platform, Gigabyte mini-PCs equipped with cheap off-the-shelf Intel 5300 Wi-Fi cards are used for the Wi-Fi transmitter and the receiver. Two antennas are attached to the receiver and one to the transmitter. We use the CSI Tool developed by Halperin et al. [22] to collect Wi-Fi CSI samples. Both the transmitter and receivers work on the 5 GHz band with a 20 MHz channel. Based on the deployment guidelines, the WiLife platform is deployed in two real home environments: Smart Home A and Smart Home B. Figure 20 shows the layouts of these two smart homes. The user interface of the platform is presented in Figure 21,

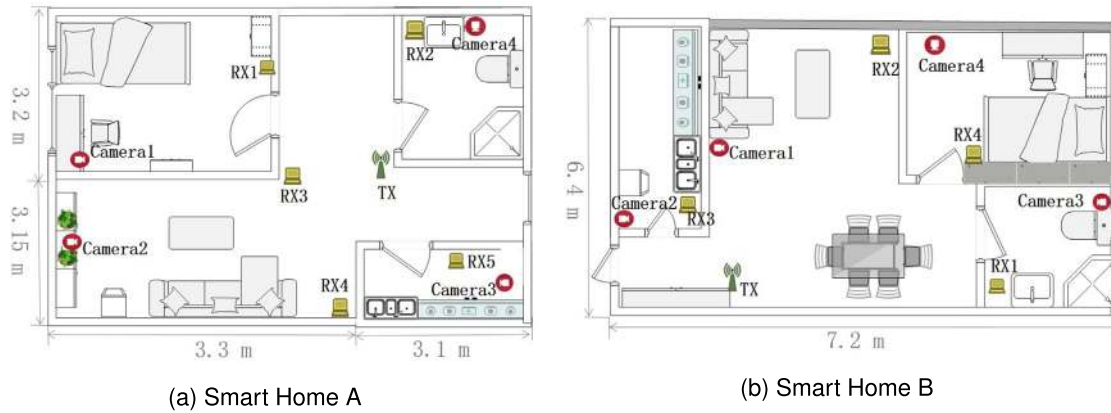


Fig. 20. Experimental environments for WiLife. One Wi-Fi transmitter and five receivers are deployed in Smart Home A. One Wi-Fi transmitter and four receivers are deployed in Smart Home B. Multiple cameras are also deployed to record the ground-truth video. In practical applications, cameras are not required.



Fig. 21. The graphical interface of a real-time system, where we can see the real-time Wi-Fi sensing results and ground-truth video.

from which we can see the real-time Wi-Fi sensing results and ground-truth video. In practical applications, cameras are not required. WiLife has been deployed in a nursing home with 12 Alzheimer's elders for over a year and has been tested by these people, from which we observed that individual diversity has little impact on the performance of WiLife. Due to privacy concerns, we cannot report those results and can only share the test results of another 15 volunteers here to show the robustness and long-term stability of the system in two different environments. Approved by IRB, all volunteers have signed an informed consent form, being aware of the experiment procedures and data usage.

3.3 Evaluation of Space Segmentation

In both environments, we asked 15 volunteers (5 females, 10 males) to perform daily activities such as cooking, dining, sleeping, watching TV, and walking around. During a 20-minute session of activities, volunteers are

	Predicted area				
		Bath-room	Hallway	Bedroom	Outdoor
Actual Area	Bath-room	0.981	0.019	0	0
	Hallway	0.011	0.963	0.014	0.012
	Bedroom	0	0.016	0.984	0
	Outdoor	0	0.013	0.012	0.975

(a)

	Predicted area					
		Bath-room	Living Room	Bed-room	Kitchen	Outdoor
Actual Area	Bath-room	0.977	0.023	0	0	0
	Living Room	0.013	0.956	0.009	0.011	0.011
	Bedroom	0	0.023	0.977	0	0
	Kitchen	0	0.018	0	0.982	0
	Outdoor	0	0.029	0	0	0.971

(b)

Fig. 22. Space segmentation result: (a) and (b) are confusion matrices for two environments.

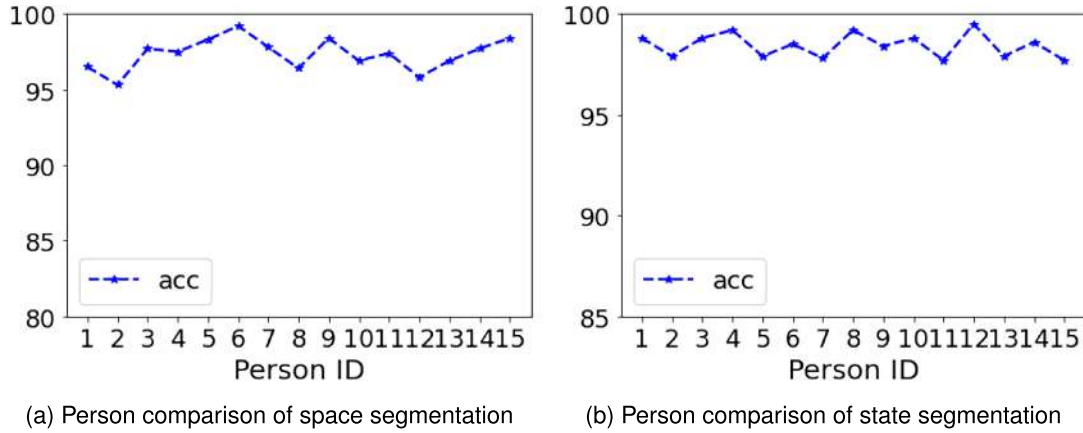


Fig. 23. Comparison for different participants. (a) and (b) are comparison results of different participants for space segmentation and state segmentation.

encouraged to carry out activities while moving across different rooms (as much as possible). It is worth noting that no activity instructions are suggested to volunteers, so they can act according to their daily habits. For each volunteer, 15 sessions of activities have been collected, with a total dataset of 4,500 minutes. These activities were recorded simultaneously by Web cameras as ground truth. During each session of activities, the volunteer can switch to any area or perform any activities as he/she will. In total, 9,952 area switches have taken place during the 4,500 minutes.

The system performance for area detection is presented in the form of a confusion matrix, as shown in Figure 22. It is worth noting that there is a transition area in each environment, through which one must pass before reaching another area, e.g., living room in Figure 20. The transition areas suffer from delays in both living room–bedroom and living room–bathroom switches. Hence, their accuracy is slightly lower than that of the other areas. Also, in the presence of such transition areas, the human target is not able to switch directly between bedroom and bathroom/kitchen. Thus, we can notice that all the mistakes in the confusion matrix are caused by switches between adjacent areas. Apart from the evaluation of different environments, we also evaluate the system against individual diversity, and the system performs consistently for different individuals as shown in Figure 23(a). Overall, the space segmentation module achieves a high area detection accuracy of up to 97.3%.

		Predicted state		
Actual state		Still	Walking	In-situ moving
	Still	0.991	0	0.009
	Walking	0	0.986	0.014
	In-situ moving	0.011	0.013	0.976

(a)

		Predicted state		
Actual state		Still	Walking	In-situ moving
	Still	0.994	0	0.006
	Walking	0	0.981	0.019
	In-situ moving	0.010	0.010	0.980

(b)

Fig. 24. State segmentation result: (a) and (b) are confusion matrices for two environments.

Table 1. Information about Volunteers

	Gender	Age	Height	Weight	In A	In B
Volunteer1	Male	25	183 cm	92 kg	–	15 D
Volunteer2	Female	27	162 cm	53 kg	15 D	–
Volunteer3	Male	34	173 cm	70 kg	15 D	–

D refers to days.

3.4 Evaluation of State Segmentation

We also evaluate the performance of the state segmentation module using the dataset collected above. In the total dataset of 4,500 minutes, 30,357 segments of different states are collected, 35% for walking, 20% for *in-situ* moving, and 45% for the still state. The performance of state segmentation is presented in Figure 24. Like transition areas, *in-situ* moving plays a role as a transition state. Thus, the walking state is not able to switch directly to the still state, resulting in zero mutual error between these two states. However, since the *in-situ* moving state can switch to each of the other two states, the accuracy is slightly lower. With regard to individual diversity, the system performances for different people are also consistent, as shown in Figure 23(b).

3.5 Evaluation of Overall Platform

To the best of our knowledge, this is the first work focusing on advancing the practical application of commodity Wi-Fi-based systems for long-term daily status in-home monitoring. To fully evaluate the overall performance of WiLife, we deployed the system in the above two real-home environments and kept it running continuously throughout the day. We invited three volunteers (see Table 1) to carry out their daily activities in these two homes. Volunteer2 and Volunteer3 each have lived in Smart Home A for 15 days, and Volunteer1 has lived in Smart Home B for 15 days. To record the ground truth, Web cameras were also installed. Moreover, we have built a Web site to visualize the long-term records of daily life status. The screenshot of the WiLife Web site is illustrated in Figure 25. To understand the daily habits of the volunteers as soon as possible, we first carefully observed the recorded videos of the volunteers during a normal day, obtaining their daily habit vectors. We further confirmed these daily habits with the volunteers in the form of questionnaires, and learned about the numerical deviations of their habits, thus constructing their habit matrices. Then, the living index can be extracted to characterize the 15 × 24 hours' daily life for each volunteer, as shown in Figure 26(a)–(c). As we can see, Volunteer1 and Volunteer3 are abnormal on the 11th and 7th day, respectively, while Volunteer2 is normal for all 15 days. In addition, considering the overall fluctuation range of the living index, the daily habits of Volunteer3 (except for the abnormal day) are more regular than those of the other two volunteers.



Fig. 25. The screenshots of the Web site for data analysis.

To further study the cause of the abnormality, we first extract the habit vector of Volunteer1 on the 11th day and Volunteer3 on the 7th day, and then calculate the normalized distance of each feature in the habit vector. As shown in Figure 27, the normalized distance of Features 12 and 13 on the 11th day of Volunteer1 is relatively large, indicating that these two features are abnormal. Based on the feature definition in the habit vector, these two features represent the percentage of moving and walking time during the day.

Then, we can compare these two features of Volunteer1 for all 15 days. As shown in Figure 28, the values of these two features are significantly lower than on other days. After reviewing the ground-truth video, we found that Volunteer1's sitting and lying time increased significantly on the 11th day. Through the return visit, we learned that Volunteer1 did get sick on the 11th day, which explains the anomalies and demonstrates the capability of our platform to detect such anomalies. Similarly, for Volunteer3, as shown in Figure 26(d), the abnormal feature represents the total time of moving during sleep, which reflects that the volunteer suffered from insomnia on the 7th night.

Through the above experiments, we demonstrated the effectiveness of the platform in describing daily routines and detecting anomalies. On one hand, a sudden change in the *living index* indicates the presence of abnormal conditions in the elderly over a 24-hour period. Our system can identify such abrupt changes and promptly notify family members or caregivers. By observing the *habit vector* for the day, they can pinpoint the specific abnormal feature and quickly take emergency measures. For example, if it is found that an elderly person has hardly any activity within a day, it may suggest that they are seriously ill or have had an accidental fall, allowing family and caregivers to quickly check on the elderly person and take emergency action. On the other hand, each feature dimension in the *habit matrix* represents a significant type of daily behavior of the elderly, which is closely related to their health status [9, 14, 59]. For instance, an increasingly late waking time may indicate a gradual decline in sleep quality, a decrease in daily walking time may suggest a decline in physical fitness or

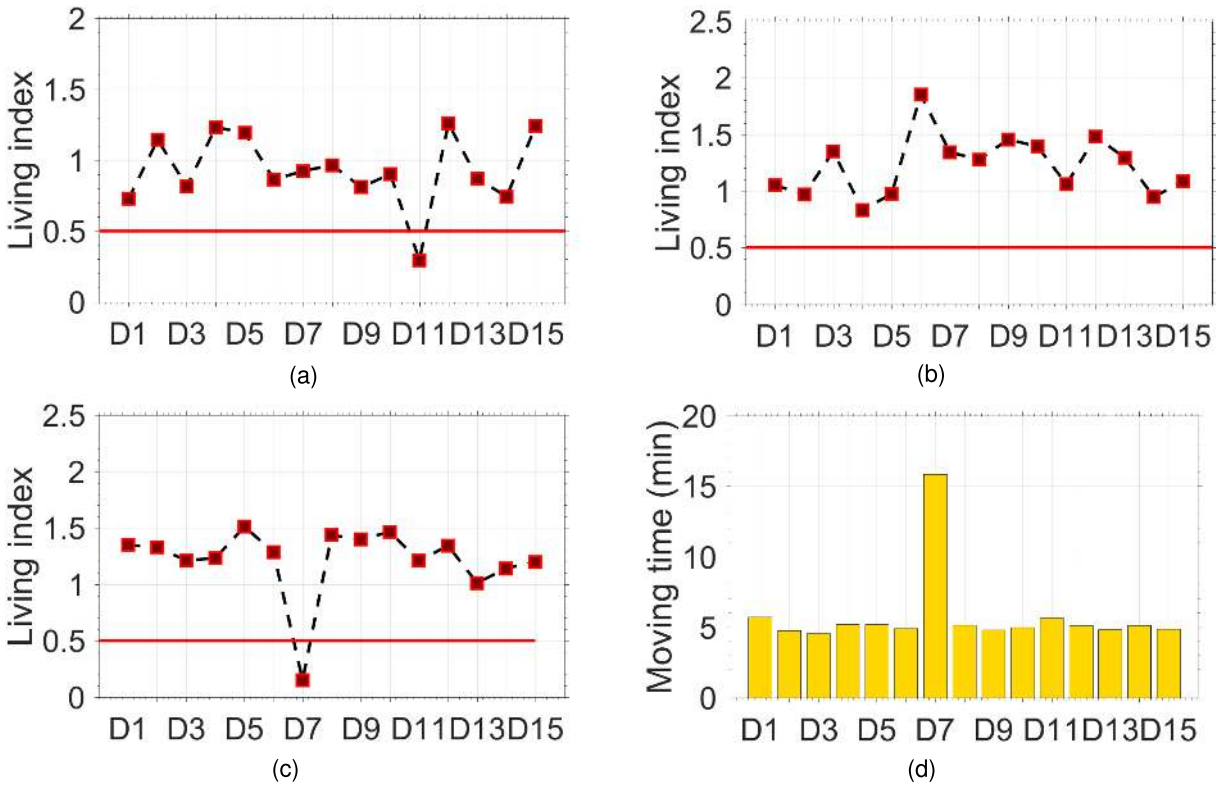


Fig. 26. (a)–(c) are living indices of Volunteer1–Volunteer3; (d) total time of moving during sleep for Volunteer3 on all days. Volunteer1 and Volunteer3 are abnormal on the 11th and 7th day, respectively, while Volunteer2 is normal for all 15 days. The total time of moving during sleep reflects that Volunteer3 suffered from insomnia on the 7th night.

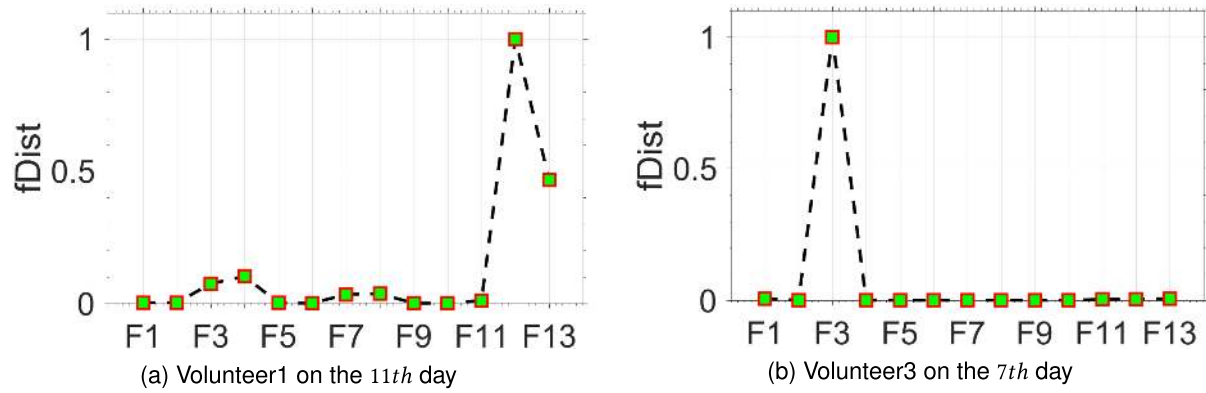


Fig. 27. Distance for features on the abnormal day (F: Feature). The distance of Features 12 and 13 on the 11th day of Volunteer1 is relatively large, which indicates the percentage of moving and walking time during the day.

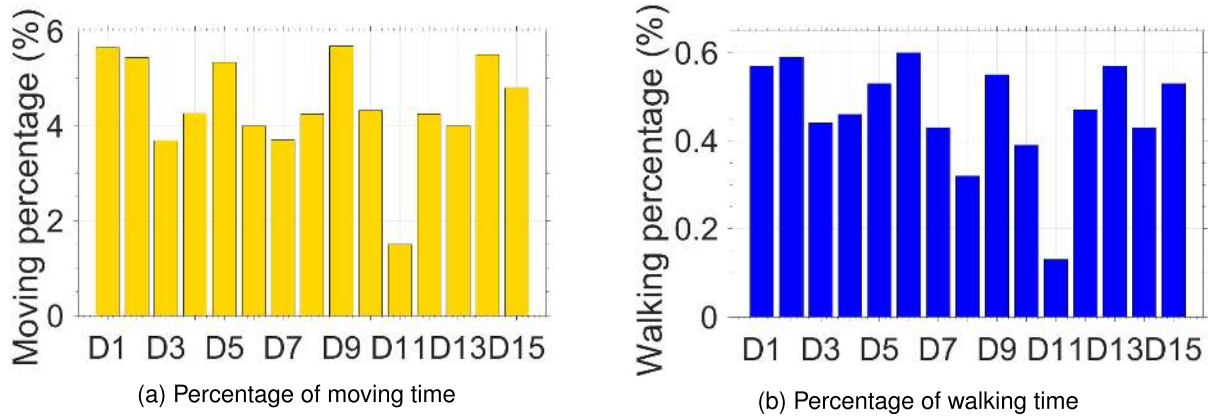


Fig. 28. Comparison for percentage of moving and walking time for all 15 days.

worsening of a condition, and an increasing frequency of bathroom visits may be related to kidney function abnormalities or urinary system infections. In other words, by observing the long-term accumulated habit matrix, doctors or health management experts can understand the long-term evolution of the daily behaviors of the elderly or illness development of chronic disease patients. When these subtle changes are captured, doctors or health managers can conduct targeted health checks on the elderly to prevent certain symptoms from developing into more serious diseases.

4 Related Work

Eldercare Techniques. The topic of eldercare has attracted increasing attention in elder living and healthcare communities. Various eldercare systems have been proposed [19, 21]. Commonly used wearable sensors include gyroscopes [33], accelerometer sensors [17], RFIDs [43], smartwatches [28], and smartphones [25]. These solutions require the subject to wear or carry such sensors all the time for continuous monitoring, which is inconvenient. Some people may be willing to sacrifice convenience for finer-grained sensing granularity. However, these techniques can only recognize a single action (e.g., fall) or activities that consist of repeating actions, such as respiration, running, and cycling. In daily life, the activities of the elderly can be diverse. Many activities are irregular and last for a long time, such as cooking and using the toilet. Even with wearable devices, these complex activities cannot be recognized. In addition, due to the limited accuracy of GPS in indoor environments, wearable devices cannot provide room-level fine-grained location information (i.e., where in the home). Therefore, these methods cannot be applied to long-term daily status monitoring of the elderly. Moreover, for long-term health monitoring of the elderly, the most important thing is to find abnormal behaviors rather than recognize a specific action. Other systems exploit the ambient information (e.g., audio noise [15], floor vibration [23, 46], infrared sensing data [27, 29]), motion, and touching [11] to achieve eldercare in a non-intrusive way. However, these systems require the deployment of dedicated devices in the environment, and sound noise and pressure around the subject in the environment might cause frequent false alarms. Another line of research uses cameras installed in the home environment [10], which is restricted by the LoS, computation cost for real-time processing, as well as privacy concerns [13]. In terms of using various radars for human sensing, Doppler radars [16] can sense human movement not fine-grained living habit information. Frequency-modulated continuous wave radars [3, 4] require a strict linear relationship between the transmission time and frequency, which is difficult to satisfy in practice. When sensing a large range or sensing through walls, ultra-wideband radars [7] require high instantaneous transmission power and introduce high costs [6]. Such radar-based techniques may work well in specific scenarios, but their current deployments are limited. In contrast, this work leverages Wi-Fi signals that

are widely available and also offers good privacy protection. Compared with the above sensing technologies, Wi-Fi devices are ubiquitous in indoor environments. Various home Wi-Fi-enabled appliances (e.g., routers, TV) form many pairs of Wi-Fi communication links. No extra infrastructure is required if the existing Wi-Fi signals can be utilized for elderly sensing.

Device-Free Sensing Using Wi-Fi. Wi-Fi signals have been explored to achieve device-free sensing with various applications. We focus on the I/O detection, localization and activity recognition systems related to our work [36, 39, 48, 53, 54, 58, 60, 61]. Wi-Fi-based I/O detectors usually achieve I/O detection by sensing human motion through Wi-Fi signals [36, 60]. However, if such motion sensing-based approach is directly applied to detect entry and exit in different areas within the same indoor environment, the motion of a person at any location inside the environment could be detected by devices in every area, making it challenging to determine the person's precise area. In contrast, our system is not only capable of functioning as an I/O detector for a house but also provides area detection within the house. This dual functionality allows for more comprehensive monitoring and enhances the utility of the system in various applications such as elderly care, security, and smart home systems. Apart from I/O detection, lots of Wi-Fi-based localization approaches attempt to obtain the fine-grained location information of the sensing target, which can be categorized into fingerprinting-based [1, 53, 61] and geometric-based [31, 39] methods. However, on the one hand, all these works require LoS-propagated communication links to reduce fluctuations in signal feature. This implies a strict deployment requirement that there must be no occlusion between any transmitter and receiver pair, which is difficult to meet in real life. On the other hand, focusing on the 90th percentile error rather than median error, current device-free human localization solutions are still as high as 2 m [5], hindering obtaining accurate location information in real-world home applications. Wi-Fi signals can also be used for human activity recognition [24, 26, 54, 58], such as fall detection [24], gesture recognition [2, 34], and exercise recognition [35]. Most existing studies [54, 58] perform two steps to achieve activity recognition: activity segmentation and activity classification. The key assumption is that the activities can be manually segmented or there is a set of pre-defined rules on actions (e.g., remaining still before and after an action). Furthermore, the mainstream activity classification methods are sensitive to the subject's location and orientation [69]. They require the user to take actions in a fixed location and even a fixed orientation. It is evident that such assumptions hinder the practicality of current activity recognition methods for long-term care of the elderly in real-life environments.

Instead of obtaining precise locations and recognizing specific activities for eldercare, this article proposes to understand the living habits and health conditions of the elderly by monitoring the spatio-temporal change patterns of their basic daily life status, including the precise area and behavioral state information at a certain time.

5 Discussion

Using Multiple Transmitters. For very large environments, a single TX may not enough to cover the entire area. In such case, multiple transmitters can be utilized. To avoid the misleading effects that might arise from signal interference from multiple transmitters, our system employs a frequency division working schema. This schema configures each transmitter (TX) to operate on a distinct channel, with receivers periodically scanning these channels to capture signals from multiple transmitters. By separating the signals in the frequency domain, the system can effectively avoid effect of signal interference, ensuring the accuracy and reliability. It's worth noting that, in addition to frequency division approach, other systems may opt for a time-division multiplexing scheme to prevent signal interference. This alternative method involves each TX transmitting signals at different time intervals, thus avoiding the possibility of signal interference.

System Inference. The impact of other moving objects (e.g., movements of pets and machines) on wireless signals depends on the effective reflection area introduced by the object [30]. Such effective reflection area is related to the dynamic object's area and their relative height to the transmitting and receiving devices. Since



Fig. 29. User interface for lightweight calibration. For example, to re-calibrate the receiver in the bedroom, the user can click the “Start” button (in “in-wall” row “bedroom” column) to take an in-wall walk for a while, and then end the walk after clicking the “End” button. Similarly, the user can also re-sample an out-wall activity through similar operations. Afterward, the system will automatically get a new threshold, thus re-calibrating itself successfully.

domestic pets are typically much smaller than the human torso and are much lower than humans, their impact on the signal is negligible compared to human activity, making it difficult to impact system performance. In terms of the inference of machines, their movements are often periodic and regular, which differ from human movement frequencies. Therefore, we can employ signal filtering techniques (e.g., band-pass filtering) to eliminate these periodic movements, reducing their impact on the system. We have added a discussion of such inferential factors to the system in the revised article.

Changes of Environments. For long-term (e.g., months or years) monitoring of daily status, we have to take into account the environmental changes that may happen. For both methods of Space Segmentation and State Segmentation, the static signals in the environment have been removed. Thus, the CSI changes caused by the physical objects (e.g., furniture) in the environment have no impact on the accuracy of both methods. In terms of Space Segmentation, its performance is only related to the occlusion of dynamic signals by walls in the environment. In other words, the performance only changes when the relative position between the transceiver and the wall changes drastically. In this case, the system needs to be re-calibrated to fit the change. To address this challenge, we have developed a lightweight automatic calibration mechanism that is integrated into the system. This mechanism facilitates user-initiated re-calibration in response to significant changes in the locations of transmitters or receivers. For instance, if the location of the receiver in the bedroom undergoes a substantial change, the user/ops can initiate a calibration process by walking inside and outside the bedroom and using the calibration interface illustrated in Figure 29 to collect the Wi-Fi CSI data in the new setting. Based on the newly collected activity data, the system can automatically adjust the segmentation threshold and thereby achieve successful re-calibration.

Multi-Person Sensing. Currently, extensive experiments have verified the effectiveness of our system for the single-person monitoring. However, for daily activities monitoring of multiple people, it still presents a significant challenge in Wi-Fi-based systems [49]. Due to the small Wi-Fi bandwidth (20 MHz), it is extremely difficult for commodity Wi-Fi devices to separate these reflected path signals and obtain the accurate number of targets. Regarding this challenge, we are actively exploring the innovative approaches to extend our system’s capabilities to multi-person monitoring. One promising direction is to obtain fine-grained **Time-of-Flight (ToF)** measurements

from Wi-Fi signals by splicing multiple channels and improving signal frequency resolution. Then, by analyzing ToF data from multiple transmitters and receivers, we can capture detailed position information of multiple individuals, helping separate the signals and dynamically select the best TX–RX pair to sense the velocity information (i.e., State) of each individual. Although these solutions are still in the research and development phase, we are optimistic about their potential to enable effective multi-person monitoring in future iterations of our system.

Further Useful Insights. Apart from informing elders’ health condition decline and abnormal situations in terms of daily status, WiLife can be further extended to enable applications such as fall detection and sleep monitoring. For example, we interestingly discovered that different sleep stages (Rapid Eye Movement Sleep, Non-Rapid Eye Movement Sleep) are accompanied by different breathing rates and body movements, which can be extracted from Wi-Fi signals, thus allowing for the possibility of fine-grained analysis of sleep conditions. With further advances in Wi-Fi sensing technology, we envision a suite of rich functionalities being developed on top of our WiLife framework for eldercare and other application domains.

6 Conclusion

Advances in ubiquitous Wi-Fi technology enable new healthcare options for the aging-in-place elderly. Numerous studies have explored the potential of using Wi-Fi signals to address urgent life safety concerns for the elderly, including fall detection and vital sign monitoring. However, apart from these acute safety issues, no work has yet addressed the need for long-term and continuous monitoring of the elderly’s daily routines, which is critical but challenging due to continuous activity segmentation and location/orientation dependencies. With the goal of supporting long-term care for the elderly, this article proposes a novel framework called WiLife. By continuously monitoring the elderly’s spatio-temporal daily status information, represented as $\langle \text{Time, Area, State} \rangle$, WiLife can offer valuable insights into when, where, and how the activities occur. Moreover, WiLife is pioneering in its approach to mine the daily habits of the elderly by integrating their spatio-temporal daily status. Based on an analysis of 45×24 hours of daily life status in real-world settings and a nursing home deployment, WiLife has demonstrated its effectiveness in characterizing users’ living habits and detecting anomalies.

References

- [1] Heba Abdel-Nasser, Reham Samir, Ibrahim Sabek, and Moustafa Youssef. 2013. MonoPHY: Mono-stream-based device-free WLAN localization via physical layer information. In *WCNC*, 4546–4551.
- [2] Heba Abdelnasser, Moustafa Youssef, and Khaled A. Harras. 2015. WiGest: A ubiquitous WiFi-based gesture recognition system. In *INFOCOM*, 1472–1480.
- [3] Fadel Adib, Zachary Kabelac, and Dina Katabi. 2015. Multi-person localization via RF body reflections. In *NSDI '15*. Oakland, CA, 279–292.
- [4] Fadel Adib, Zach Kabelac, Dina Katabi, and Robert C. Miller. 2014. 3D tracking via body radio reflections. In *NSDI '14*. USENIX Association, Seattle, WA, 317–329.
- [5] Fakhrul Alam, Nathaniel Faulkner, and Baden Parr. 2021. Device-Free Localization: A Review of Non-RF Techniques for Unobtrusive Indoor Positioning. *IEEE Internet of Things Journal* 8, 6 (2021), 4228–4249. DOI: <https://doi.org/10.1109/JIOT.2020.3030174>
- [6] Abdulrahman Alarifi, AbdulMalik Al-Salman, Mansour Alsaleh, Ahmad Alnafessah, Suheer Al-Hadhrani, Mai A. Al-Ammar, and Hend S. Al-Khalifa. 2016. Ultra Wideband Indoor Positioning Technologies: Analysis and Recent Advances. *Sensors (Basel, Switzerland)* 16, 5 (2016), 707.
- [7] Boyd Anderson, Mingqian Shi, Vincent Y. F. Tan, and Ye Wang. 2019. Mobile Gait Analysis Using Foot-Mounted UWB Sensors. *Proceedings of the ACM on Interactive, Mobile, Wearable and Ubiquitous Technologies* 3, 3, Article 73 (Sep. 2019), 22 pages.
- [8] Taxiarchis Botsis and Gunnar Hartvigsen. 2008. Current Status and Future Perspectives in Telecare for Elderly People Suffering from Chronic Diseases. *Journal of Telemedicine and Telecare* 14, 4 (2008), 195–203.
- [9] Evgeniy Bryndin and Irina Bryndina. 2017. Formation of Public Health Care on Basis of Healthy Lifestyle. *International Journal of Psychological and Brain Sciences* 2, 3 (2017), 63–68. DOI: <https://doi.org/10.11648/j.jpbs.20170203.11>
- [10] Q. Cai and J. K. Aggarwal. 1998. Automatic tracking of human motion in indoor scenes across multiple synchronized video streams. In *ICCV*, 356–362.

- [11] Loïc Caroux, Charles Consel, Lucile Dupuy, and Hélène Sauzéon. 2014. Verification of daily activities of older adults: A simple, non-intrusive, low-cost approach. In *ASSETS '14*. ACM, New York, NY, 43–50.
- [12] Richard Hedley Clarke. 1968. A Statistical Theory of Mobile-Radio Reception. *The Bell System Technical Journal* 47, 6 (July 1968), 957–1000.
- [13] George Demiris, Debra Oliver, Jarod Giger, Marjorie Skubic, and Marilyn Rantz. [n.d.]. Older Adults' Privacy Considerations for Vision Based Recognition Methods of Eldercare Applications. *Technology and Health Care* 17, 1 (Jan 2009), 41–48.
- [14] William H. Dietz. 1996. The Role of Lifestyle in Health: The Epidemiology and Consequences of Inactivity. *Proceedings of the Nutrition Society* 55, 3 (1996), 829–840. DOI: <https://doi.org/10.1079/PNS19960082>
- [15] Thilina Dissanayake, Takuya Maekawa, Daichi Amagata, and Takahiro Hara. 2018. Detecting Door Events Using a Smartphone via Active Sound Sensing. *Proceedings of the ACM on Interactive, Mobile, Wearable and Ubiquitous Technologies* 2, 4, Article 160 (Dec. 2018), 26 pages.
- [16] D. P. Fairchild and R. M. Narayanan. 2016. Multistatic Micro-Doppler Radar for Determining Target Orientation and Activity Classification. *IEEE Transactions on Aerospace and Electronic Systems* 52, 1 (2016), 512–521.
- [17] F. Foerster, M. Smeja, and J. Fahrenberg. 1999. Detection of Posture and Motion by Accelerometry: A Validation Study in Ambulatory Monitoring. *Computers in Human Behavior* 15, 5 (1999), 571–583.
- [18] Ruiyang Gao, Mi Zhang, Jie Zhang, Yang Li, Enze Yi, Dan Wu, Leye Wang, and Daqing Zhang. 2021. Towards Position-Independent Sensing for Gesture Recognition with Wi-Fi. *Proceedings of the ACM on Interactive, Mobile, Wearable and Ubiquitous Technologies* 5, 2, Article 61 (Jun. 2021), 28 pages. DOI: <https://doi.org/10.1145/3463504>
- [19] Kathrin Gerling, Mo Ray, Vero Vanden Abeele, and Adam B. Evans. 2020. Critical Reflections on Technology to Support Physical Activity among Older Adults: An Exploration of Leading HCI Venues. *ACM Transactions on Accessible Computing* 13, 1, Article 1 (Apr. 2020), 23 pages.
- [20] Wei Gong and Jiangchuan Liu. 2018. SiFi: Pushing the Limit of Time-Based WiFi Localization Using a Single Commodity Access Point. *Proceedings of the ACM on Interactive, Mobile, Wearable and Ubiquitous Technologies* 2, 1 (Mar 2018), Article 10, 21 pages.
- [21] Abhay Gupta, Kuldeep Gupta, Kshama Gupta, and Kapil Gupta. 2020. A survey on human activity recognition and classification. In *ICCSPP*, 0915–0919.
- [22] Daniel Halperin, Wenjun Hu, Anmol Sheth, and David Wetherall. 2011. Tool Release: Gathering 802.11N Traces with Channel State Information. *SIGCOMM Computer Communication Review* 41, 1 (Jan. 2011), 53–53.
- [23] J. Hamilton, B. Joyce, M. Kasarda, and Pablo Tarazaga. 2014. *Characterization of Human Motion through Floor Vibration*. In *Conference Proceedings of the Society for Experimental Mechanics Series*. F. Catbas (Ed.), Dynamics of Civil Structures, Vol. 4, Springer, Cham.
- [24] Chunmei Han, Kaishun Wu, Yuxi Wang, and Lionel M. Ni. 2014. WiFall: Device-free fall detection by wireless networks. In *INFOCOM*, 581–594.
- [25] Tian Hao, Guoliang Xing, and Gang Zhou. 2015. RunBuddy: A smartphone system for running rhythm monitoring. In *UBICOMP*, 133–144.
- [26] Wenjun Jiang, Chenglin Miao, Fenglong Ma, Shuochao Yao, Yaqing Wang, Ye Yuan, Hongfei Xue, Chen Song, Xin Ma, Dimitrios Koutsonikolas, Wenyao Xu, and Lu Su. 2018. Towards environment independent device free human activity recognition. In *MOBICOM*, 289–304.
- [27] Ju Han and B. Bhanu. 2005. Human activity recognition in thermal infrared imagery. In *CVPR*, 17–17.
- [28] Young-Ho Kim, Diana Chou, Bongshin Lee, Margaret Danilovich, Amanda Lazar, David E. Conroy, Hernisa Kacorri, and Eun Kyoung Choe. 2022. MyMove: Facilitating older adults to collect in-situ activity labels on a smartwatch with speech. In *CHI '22*. ACM, New York, NY, Article 416, 21 pages.
- [29] Simon Klakegg, Jorge Goncalves, Chu Luo, Aku Visuri, Alexey Popov, Niels van Berkel, Zhanna Sarsenbayeva, Vassilis Kostakos, Simo Hosio, Scott Savage, Alexander Bykov, Igor Meglinski, and Denzil Ferreira. 2018. Assisted Medication Management in Elderly Care Using Miniaturised Near-Infrared Spectroscopy. *Proceedings of the ACM on Interactive, Mobile, Wearable and Ubiquitous Technologies* 2, 2, Article 69 (July 2018), 24 pages.
- [30] Eugene F. Knott, John F. Schaeffer, and Michael T. Tully. 2004. *Radar Cross Section*. SciTech Publishing.
- [31] Manikanta Kotaru, Kiran Joshi, Dinesh Bharadia, and Sachin Katti. 2015. SpotFi: Decimeter level localization using Wi-Fi. In *SIFCOMM*, 269–282.
- [32] Kevin C. Kregel and Hannah J. Zhang. 2007. An Integrated View of Oxidative Stress in Aging: Basic Mechanisms, Functional Effects, and Pathological Considerations. *American Journal of Physiology-Regulatory, Integrative and Comparative Physiology* 292, 1 (2007), R18–R36.
- [33] Oscar D. Lara and Miguel A. Labrador. 2013. A Survey on Human Activity Recognition Using Wearable Sensors. *IEEE Communications Surveys Tutorials* 15, 3 (2013), 1192–1209.
- [34] Hong Li, Wei Yang, Jianxin Wang, Yang Xu, and Liusheng Huang. 2016. WiFinger: Talk to your smart devices with finger-grained gesture. In *UBICOMP*, 250–261.
- [35] Shengjie Li, Xiang Li, Qin Lv, Guiyu Tian, and Daqing Zhang. 2018. WiFit: Ubiquitous bodyweight exercise monitoring with commodity Wi-Fi devices. In *UIC*, 530–537.

- [36] Shengjie Li, Xiang Li, Kai Niu, Hao Wang, Yue Zhang, and Daqing Zhang. 2017. AR-Alarm: An adaptive and robust intrusion detection system leveraging CSI from commodity Wi-Fi. In *ICOST*, 211–223.
- [37] S. Li, Z. Liu, Y. Zhang, Q. Lv, and D. Zhang. 2020. WiBorder: Precise Wi-Fi Based Boundary Sensing via Through-Wall Discrimination. *Proceedings of the ACM on Interactive, Mobile, Wearable and Ubiquitous Technologies* 4, 3 (Sep 2020), Article 89, 30 pages.
- [38] Seon-Woo Lee Li and K. Mase. 2002. Activity and Location Recognition Using Wearable Sensors. *IEEE Pervasive Computing* 1, 3 (July 2002), 24–32.
- [39] Xiang Li, Shengjie Li, Daqing Zhang, Jie Xiong, Yasha Wang, and Hong Mei. 2016. Dynamic-MUSIC: Accurate device-free indoor localization. In *UBICOMP*, 196–207.
- [40] Xiang Li, Daqing Zhang, Qin Lv, Jie Xiong, Shengjie Li, Yue Zhang, and Hong Mei. 2017. IndoTrack: Device-Free Indoor Human Tracking with Commodity Wi-Fi. *Proceedings of the ACM on Interactive, Mobile, Wearable and Ubiquitous Technologies* 1, 3 (Sep 2017), Article 72, 22 pages.
- [41] Xiang Li, Daqing Zhang, Jie Xiong, Yue Zhang, Shengjie Li, Yasha Wang, and Hong Mei. 2018. Training-Free Human Vitality Monitoring Using Commodity Wi-Fi Devices. *Proceedings of the ACM on Interactive, Mobile, Wearable and Ubiquitous Technologies* (2018) 2, 3 (Sep 2018), Article 121, 25 pages.
- [42] Xuefeng Liu, Jiannong Cao, Shaojie Tang, Jiaqi Wen, and Peng Guo. 2016. Contactless Respiration Monitoring Via Off-the-Shelf WiFi Devices. *IEEE Transactions on Mobile Computing* 15, 10 (Oct. 2016), 2466–2479.
- [43] Yunhao Liu, Yiyang Zhao, Lei Chen, Jian Pei, and Jinsong Han. 2007. Mining Frequent Trajectory Patterns for Activity Monitoring Using Radio Frequency Tag Arrays. In *Fifth Annual IEEE International Conference on Pervasive Computing and Communications (PerCom'07)*, White Plains, NY, 37–46.
- [44] R. D. Maesschalck, D. Jouan-Rimbaud, and D. L. Massart. 2000. The Mahalanobis Distance. *Chemometrics and Intelligent Laboratory Systems* 50 (2000), 1–18.
- [45] J. James Banks, R. Blundell, M. Marmot, C. Lessof, and J. Nazroo. 2003. Health, wealth and lifestyles of the older population in England. In *The 2002 English Longitudinal Study of Ageing*. PNAS.
- [46] Robert J. Orr and Gregory D. Abowd. 2000. The smart floor: A mechanism for natural user identification and tracking. In *CHI '00*, 275–276.
- [47] A. P. Porsteinsson, R. S. Isaacson, Sean Knox, M. N. Sabbagh, and Rubino I. 2021. Diagnosis of Early Alzheimer's Disease: Clinical Practice in 2021. *The Journal of Prevention of Alzheimer's Disease* 8, 3 (2021), 71–386.
- [48] Kun Qian, Chenshu Wu, Zheng Yang, Yunhao Liu, and Kyle Jamieson. 2017. Widar: Decimeter-level passive tracking via velocity monitoring with commodity Wi-Fi. In *Mobihoc '17*. ACM, New York, NY, Article 6, 10 pages.
- [49] Sheng Tan, Yili Ren, Jie Yang, and Yingying Chen. 2022. Commodity WiFi Sensing in Ten Years: Status, Challenges, and Opportunities. *IEEE Internet of Things Journal* 9 (Sep. 2022), 1–1. DOI: <https://doi.org/10.1109/JIOT.2022.3164569>
- [50] P. Teo, K. Mehta, L. L. Thang, and A. Chan. 2006. *Ageing in Singapore*. Taylor and Francis. Retrieved from <https://www.perlego.com/book/1710244/ageing-in-singapore-service-needs-and-the-state-pdf>
- [51] Hao Wang, Daqing Zhang, Junyi Ma, Yasha Wang, Yuxiang Wang, Dan Wu, Tao Gu, and Bing Xie. 2016. Human respiration detection with commodity Wifi devices: Do user location and body orientation matter? In *UBICOMP '16*. ACM, New York, NY, 25–36.
- [52] Hao Wang, Daqing Zhang, Yasha Wang, Junyi Ma, Yuxiang Wang, and Shengjie Li. 2017. RT-Fall: A Real-Time and Contactless Fall Detection System with Commodity WiFi Devices. *IEEE Transactions on Mobile Computing* 16, 2 (Feb. 2017), 511–526.
- [53] Ju Wang, Hongbo Jiang, Jie Xiong, Kyle Jamieson, Xiaojiang Chen, Dingyi Fang, and Binbin Xie. 2016. LiFS: Low human-effort, device-free localization with fine-grained subcarrier information. In *MOBICOM*, 2550–2563.
- [54] Wei Wang, Alex X. Liu, Muhammad Shahzad, Kang Ling, and Sanglu Lu. 2015. Understanding and modeling of Wi-Fi signal based human activity recognition. In *MOBICOM*, 65–76.
- [55] Xuyu Wang, Yang Chao, and Shiwen Mao. 2017. PhaseBeat: Exploiting CSI phase data for vital sign monitoring with commodity WiFi devices. In *ICDCS*, 1230–1239.
- [56] Xuanzhi Wang, Kai Niu, Jie Xiong, Bocheng Qian, Zhiyun Yao, Tairong Lou, and Daqing Zhang. 2022. Placement Matters: Understanding the Effects of Device Placement for WiFi Sensing. *Proceedings of the ACM on Interactive, Mobile, Wearable and Ubiquitous Technologies* 6, 1, Article 32 (Mar. 2022), 25 pages. DOI: <https://doi.org/10.1145/3517237>
- [57] Xuyu Wang, Chao Yanc, and Shiwei Mao. 2018. TensorBeat: Tensor Decomposition for Monitoring Multiperson Breathing Beats with Commodity WiFi. *ACM Transactions on Intelligent Systems and Technology* 9, 1 (2018), 8.1–8.27.
- [58] Yan Wang, Jian Liu, Yingying Chen, Marco Gruteser, Jie Yang, and Hongbo Liu. 2014. E-eyes: Device-free location-oriented activity identification using fine-grained WiFi signatures. In *MOBICOM*, 617–628.
- [59] J. H. Weisburger. 2002. Lifestyle, Health and Disease Prevention: The Underlying Mechanisms. *European Journal of Cancer Prevention* 11 (2002), S1–S7. DOI: <http://www.jstor.org/stable/45051291>
- [60] Chenshu Wu, Zheng Yang, Zimu Zhou, Xuefeng Liu, Yunhao Liu, and Jiannong Cao. 2015. Non-Invasive Detection of Moving and Stationary Human with WiFi. *IEEE Journal on Selected Areas in Communications* 33, 11 (2015), 2329–2342. DOI: <https://doi.org/10.1109/JSAC.2015.2430294>
- [61] Kaishun Wu, Jiang Xiao, Youwen Yi, Min Gao, and Lionel M. Ni. 2012. FILA: Fine-grained indoor localization. In *INFOCOM*, 2210–2218.

- [62] Yang Xu, Wei Yang, Jianxin Wang, Xing Zhou, Hong Li, and Liusheng Huang. 2018. WiStep: Device-Free Step Counting with WiFi Signals. *Proceedings of the ACM on Interactive, Mobile, Wearable and Ubiquitous Technologies* 1, 4, Article 172 (Jan. 2018), 23 pages.
- [63] H. Yan, Y. Zhang, Y. Wang, and K. Xu. 2020. WiAct: A Passive WiFi-Based Human Activity Recognition System. *IEEE Sensors Journal* 20, 1 (2020), 296–305.
- [64] Zheng Yang, Zimu Zhou, and Yunhao Liu. 2013. From RSSI to CSI: Indoor Localization via Channel Response. *ACM Computing Surveys* 46, 2, Article 25 (Dec. 2013), 32 pages.
- [65] Xinguo Yu. 2008. Approaches and principles of fall detection for elderly and patient. In *HealthCom '08*.
- [66] Youwei Zeng, Dan Wu, Jie Xiong, Jinyi Liu, Zhaopeng Liu, and Daqing Zhang. 2020. MultiSense: Enabling Multi-Person Respiration Sensing with Commodity WiFi. *Proceedings of the ACM on Interactive, Mobile, Wearable and Ubiquitous Technologies* 4, 3, Article 102 (Sep. 2020), 29 pages.
- [67] Youwei Zeng, Dan Wu, Jie Xiong, Enze Yi, Ruiyang Gao, and Daqing Zhang. 2019. FarSense: Pushing the Range Limit of WiFi-Based Respiration Sensing with CSI Ratio of Two Antennas. *Proceedings of the ACM on Interactive, Mobile, Wearable and Ubiquitous Technologies* 3, 3, Article 121 (Sep. 2019), 26 pages. DOI: <https://doi.org/10.1145/3351279>
- [68] Daqing Zhang, Niu Kai, Jie Xiong, Fusang Zhang, and Shengjie Li. 2021. Location Independent Vital Sign Monitoring and Gesture Recognition Using Wi-Fi. In *Contactless Human Activity Analysis*. M. A. R. Ahad, U. Mahbub, and T. Rahman (Eds.), Intelligent Systems Reference Library, Vol. 200, Springer, Cham, 185–202.
- [69] D. Zhang, H. Wang, and D. Wu. 2017. Toward Centimeter-Scale Human Activity Sensing with Wi-Fi Signals. *Computer* 50, 1 (2017), 48–57.

Received 28 September 2023; revised 21 March 2024; accepted 5 August 2024